DEPARTMENT OF DEFENCE
DEFENCE SCIENCE & TECHNOLOGY ORGANISATION | **DSTO**

The Spectrum of Electromagnetic Scatter from an Ensemble of Bodies with Angular Periodicity, as a Model for Jet Engine Modulation

John Cashman

DSTO-GD-0272

20010718 103

The Spectrum of Electromagnetic Scatter from an Ensemble of Bodies with Angular Periodicity, as a Model for Jet Engine Modulation

John Cashman
Department of Electrical Engineering, University of NSW

under contract for

Surveillance Systems Division
Electronics and Surveillance Research Laboratory

DSTO-GD-0272

ABSTRACT

A rotating ensemble of bodies of arbitrary shape with angular periodicity scatters an electromagnetic wave to produce a spectrum of frequency components characteristic of the structure and its rotation. The spectrum and its properties are predicted through electromagnetic field theory.
The theory has been developed such as to exploit the angular periodicity and therefore reduce the computational load by a large factor. A consequence of the approach is that the spectrum is found directly.
Many of the predictions have been confirmed by direct computation of the scattered field for a series of rotational positions to simulate a time series, followed by a discrete Fourier transforming to produce the spectrum.

RELEASE LIMITATION

Approved for public release

DEPARTMENT OF DEFENCE **DSTO**
DEFENCE SCIENCE & TECHNOLOGY ORGANISATION

AQ FOI-10-1776

APPROVED FOR PUBLIC RELEASE

CONTENTS

Abstract:

A rotating ensemble of bodies of arbitrary shape with angular periodicity scatters an electromagnetic wave to produce a spectrum of frequency components characteristic of the structure and its rate of rotation. The spectrum and its properties are predicted through electromagnetic field theory.

The theory has been developed such as to exploit the angular periodicity and thereby reduce the computational load by a large factor. A consequence of the approach is that the spectrum is found directly.

Many of the predictions have been confirmed by direct computation of the scattered field for a series of rotational positions to simulate a time series, followed by discrete Fourier transforming to produce the spectrum.

1. Introduction

The intake of the jet engines of an aircraft makes a major contribution to its radar cross-section. The rotation of the engine compressor, each stage of which exhibits angular periodicity, gives this contribution a distinctive spectrum by means of which one might hope to identify the target [2,3,4]. In a previous study [5] the compressor stage was crudely modelled as a coplanar ensemble of wires radiating from an axis. In the present study this is generalised by replacing each wire by a conducting body of arbitrary shape. The ensemble of bodies exhibits the same angular perodicity as did the wires. If each body is given the shape of a compressor blade a stage of the compressor may be simulated. The central hub or axle from which the blades radiate may be included without difficulty.

In the previous study a number of conclusions were drawn about the characteristics of the spectrum. These were based on the wire model, although in most cases it was intuitively clear that they would be valid for the more general case. In the present study these intuitions are established rigorously.

This study, like the previous, had two principal goals. The first was to find a means to calculate the field which exploited the periodicity of the ensemble and thereby to reduce the computation load. The second was to express the result as a frequency spectrum. In the event, the means by which the first goal was met automatically met the second.

The incident electric field is expressed as a summation of harmonics of the azimuthal angle (measured around the axis). This approach exploits the angular periodicity of the ensemble of bodies. Each harmonic of the field excites a harmonic component of the current. For each harmonic it is found necessary to calculate the current on only one body, for only one azimuthal angle of incidence; the currents on the other bodies, for other directions of incidence, are found simply from the first. In consequence, the computation needed to solve for the scattered field is reduced (compared to a direct calculation which does not exploit the angular periodicity) approximately in proportion to the number of bodies.

A further beneficial consequence of the harmonic decomposition of the incident field is that the scattered field is found directly as a frequency spectrum. The components are lines at intervals of the rotation rate multiplied by the number of bodies. This is

consistent with the fact that the ensemble re-presents the same aspect to the radar at this rate. The spectrum extends with significant strength above and below the illumination frequency by an amount equal to the Doppler shift associated with the maximum linear velocity of the bodies. Beyond these limits the spectral lines continue, becoming weaker approximately exponentially.

Many features of the spectrum of the scattered field, including those mentioned in the foregoing paragraph, may be deduced from the form of the equations without proceeding to their solution. At this point in the study, exact solutions have not been calculated. It is to be expected that further features useful for target identification may be exposed by the exact numerical solutions. To this end an approach to numerical solution has been examined and described in detail.

It is possible to make predictions concerning the effects of conditions outside the present simulation, such as the presence of the engine cowling, the presence of multiple stages and the presence of stator blades in the engine. The fact that the compressor stage is surrounded by a cowling and not in free space implies that the incident field is not a plane wave: however the true field may be decomposed into a spectrum of plane waves, each of which interacts with the scatterer in the manner described by the present theory. The presence of multiple stages has the result that the scattered field has a spectrum which has some of the character of a superposition of the spectra of the separate stages, with weaker components at intervals of the shaft rate. The presence of stator blades does not alter the frequencies of the spectrum, but, by introducing new mechanisms of electromagnetic interaction between moving and stationary bodies, causes the spectrum to have significant strength at frequencies beyond the Doppler limits mentioned above.

Many of the predictions and expectations arising from the theory have been confirmed through numerical simulation. Calculations for simple shapes have been made using the NEC program [6] for a series of angular positions and the results submitted to a fast Fourier transform. Confirmation has also been obtained through measurement of some wire structures.

2. The ensemble of bodies

In this section is described the geometry of the ensemble of bodies, together with the coordinate systems and some special parameters to be used below.

I conducting bodies, with surfaces S_i, $i=0,1,...,I-1$, are arranged about an axis (in the coordinate system to be used, the z axis) at angular spacings of $\frac{2\pi}{I}$, see figure 2.1. Their shapes are the same and oriented such that S_i is generated by rotating S_0 about the z axis throught the azimutal angle

$$\Phi_i = i\frac{2\pi}{I}. \tag{2.1}$$

The objects may be detached, as shown, or attached to one another. In the latter case the individual bodies must be defined by an arbitrary cut through the common region.

Rectangular, cylindrical and spherical coordinates will be used as convenient; the system in use will usually be apparent from the conventional symbols: (x,y,z), (ρ,ϕ,z), (r,θ,ϕ).

If a point on surface S_0 has position vector and coordinates

$$\bar{r}_0 \equiv (x_0,y_0,z_0) \equiv (\rho_0,\phi_0,z_0) \equiv (r_0,\theta_0,\phi_0),$$

with the conventional relations

$$\rho_0 = (x_0^2 + y_0^2)^{\frac{1}{2}}, \ \phi_0 = \cos^{-1}\frac{x_0}{\rho_0} = \sin^{-1}\frac{y_0}{\rho_0},$$

$$r_0 = (x_0^2 + y_0^2 + z_0^2)^{\frac{1}{2}}, \ \theta_0 = \cos^{-1}\frac{z_0}{r_0} = \sin^{-1}\frac{\rho_0}{r_0} \tag{2.2}$$

then a point of position vector

$$\bar{r}_i \equiv (\rho_i,\phi_i,z_i)$$

with

$$\rho_i = \rho_0, \ \phi_i = \phi_0 + \Phi_i, \ z_i = z_0 \tag{2.3}$$

lies on S_i.

4

Points related like $\bar{r}_0$ and $\bar{r}_i$ will be called "corresponding points". Such points are illustrated in figure 2.2. Wherever $\bar{r}_0$ and $\bar{r}_i$ or their similarly subscripted coordinates appear in the same equation, they are to be understood as corresponding in this sense.
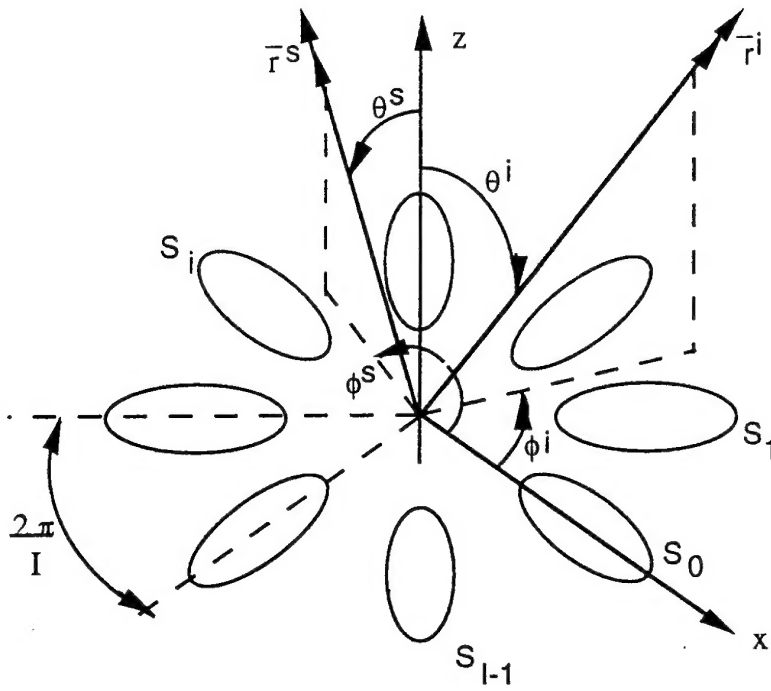
Figure 2.1: The ensemble of bodies with surfaces S_0, S_1,...S_{I-1}, disposed with angular periodicity about the z axis. A plane wave is incident from the direction of spherical coordinates θ^i,ϕ^i. The scattered field is observed from the direction θ^s,ϕ^s.

Figure 2.2: "Corresponding" points $\bar{r}_0$ and $\bar{r}_i$ on bodies S_0 and S_i. The vectors $\bar{c}_n^i(\bar{r}_0)$ and $\bar{c}_n^i(\bar{r}_i)$ are rotated relatively to one another about the z axis in the same way as $\bar{r}_0$ and $\bar{r}_i$.

3.   The incident field and its harmonics

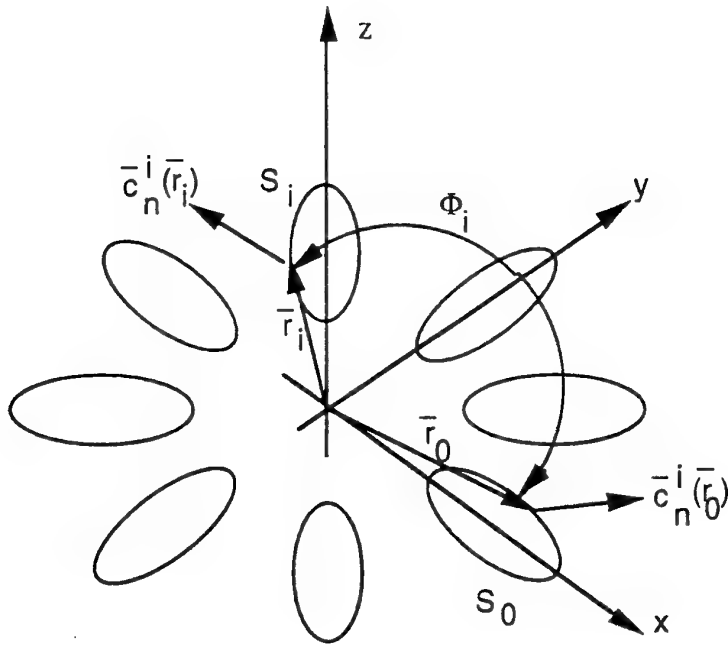In this section the incident electromagnetic field is defined.   The manner of its decomposition into a Fourier series is described and the rotation dyadic is introduced.

A plane wave is incident on the ensemble of scatterers from the direction θ^i, ϕ^i, see figure 2.1.   The electric field vector at a point (x,y,z) or (ρ,ϕ,z) is

$$\overline{E}^i = \hat{e}^i E_0 e^{jk_0(x\sin\theta^i\cos\phi^i + y\sin\theta^i\sin\phi^i + z\cos\theta^i)}$$

$$= \hat{e}^i E_0 e^{jk_0(\rho\sin\theta^i\cos(\phi-\phi^i) + z\cos\theta^i)}$$

$$(3.1)$$

where k_0 is the wave number for $e^{j\omega_0 t}$ time dependence, the factor $e^{j\omega_0 t}$ is suppressed, and $\hat{e}^i$ is a unit vector specifying the polarisation.   In this work we consider the two cases $\hat{e}^i = \hat{\theta}^i$ and $\hat{e}^i = \hat{\phi}^i$.   Any other $\hat{e}^i$ may be resolved into components in these directions.   We note

$$\hat{\theta}^i = \hat{x}\cos\theta^i\cos\phi^i + \hat{y}\cos\theta^i\sin\phi^i - \hat{z}\sin\theta^i$$

$$= \hat{\rho}\cos\theta^i\cos(\phi-\phi^i) - \hat{\phi}\cos\theta^i\sin(\phi-\phi^i) - \hat{z}\sin\theta^i$$

$$(3.2)$$

and

$$\hat{\phi}^i = -\hat{x}\sin\phi^i + \hat{y}\cos\phi^i$$

$$= \hat{\rho}\sin(\phi-\phi^i) + \hat{\phi}\cos(\phi-\phi^i)$$

$$(3.3)$$

in which the unit vectors $\hat{\rho}$ and $\hat{\phi}$ are evaluated at the observation point (ρ,ϕ,z).   Here and subsequently the superscript i specifies the incident field while the subscript i is an index specifying the body S_i.

(1), (2) and (3) give, for $\hat{e}^i = \hat{\theta}^i$

$$\bar{E}^i = (\hat{\rho}\cos\theta^i\cos(\phi-\phi^i)e^{jk_0\rho\sin\theta^i\cos(\phi-\phi^i)}$$

$$-\hat{\phi}\cos\theta^i\sin(\phi-\phi^i)e^{jk_0\rho\sin\theta^i\cos(\phi-\phi^i)}$$

$$-\hat{z}\sin\theta^i E_0 e^{jk_0\rho\sin\theta^i\cos(\phi-\phi^i)})E_0 e^{jk_0 z\cos\theta^i}$$

$$(3.4)$$

and for $\hat{e}^i = \hat{\phi}^i$

$$\bar{E}^i = (\hat{\rho}\sin(\phi-\phi^i)e^{jk_0\rho\sin\theta^i\cos(\phi-\phi^i)}$$

$$+\hat{\phi}\cos(\phi-\phi^i)e^{jk_0\rho\sin\theta^i\cos(\phi-\phi^i)}E_0 e^{jk_0 z\cos\theta^i}$$

$$(3.5)$$

The products of trigonometric and complex exponential functions in (3.4) and (3.5) are expanded, using the formulas in Appendix A, as Fourier series in $\phi-\phi^i$. Thus

$$\bar{E}^i(\bar{r}) = \sum_{n=-\infty}^{\infty} \bar{E}_n^i(\bar{r}) \tag{3.6}$$

where

$$\bar{E}_n^i(\bar{r}) = E_0 \bar{c}_n^i(\bar{r})e^{jn(\phi-\phi^i)} \tag{3.7}$$

will be referred to as the "n th harmonic" of $\bar{E}^i$, and for $\hat{e}^i = \hat{\theta}^i$,

$$\bar{c}_n^i(\bar{r}) = \bar{c}_n^{i\theta}(\bar{r})$$

$$= j^n(-\hat{\rho}\cos\theta^i j J_n'(P^i) - \hat{\phi}\cos\theta^i \frac{n}{P^i}J_n(P^i) - \hat{z}\sin\theta^i J_n(P^i))e^{jk_0 z\cos\theta^i}$$

$$(3.8)$$

while for $\hat{e}^i = \hat{\phi}^i$,

$$\bar{c}_n^i(\bar{r}) = \bar{c}_n^{i\phi}(\bar{r}) = -j^n(\hat{\rho}\frac{n}{P^i}J_n(P^i) + \hat{\phi}j J_n'(P^i))e^{jk_0 z\cos\theta^i} \tag{3.9}$$

in which

$$P^i = k_0 \rho \sin \theta^i, \tag{3.10}$$

and the non-constant unit vectors $\hat{\rho}$ and $\hat{\phi}$ are evaluated at $\bar{r}$.

Consider corresponding points $\bar{r}_0$ and $\bar{r}_i$ and the vectors $\bar{c}_n^i(\bar{r}_0)$ and $\bar{c}_n^i(\bar{r}_i)$, see figure 2.2. The position vectors are related through

$$\bar{r}_i = \bar{r}_0 \cdot \overline{\overline{R}}_i \tag{3.11}$$

where $\overline{\overline{R}}_i$ is a dyadic which rotates a vector about the z axis through angle Φ_i. In rectangular coordinates (3.11) corresponds to the matrix equation

$$\begin{bmatrix} r_{ix} \\ r_{iy} \\ r_{iz} \end{bmatrix} = \begin{bmatrix} \cos\Phi_i & -\sin\Phi_i & 0 \\ \sin\Phi_i & \cos\Phi_i & 0 \\ 0 & 0 & 1 \end{bmatrix} \begin{bmatrix} r_{0x} \\ r_{0y} \\ r_{0z} \end{bmatrix} \tag{3.12}$$

where r_{ix} etc are the rectangular components of $\bar{r}_i$. From their definitions in (3.8) and (3.19) it is clear that the $\bar{c}_n^i$ are related similarly:

$$\bar{c}_n^i(\bar{r}_i) = \bar{c}_n^i(\bar{r}_0) \cdot \overline{\overline{R}}_i \tag{3.13}$$

and with (3.7) that the harmonic fields are related by

$$\overline{E}_n^i(\bar{r}_i) = \overline{E}_n^i(\bar{r}_0) \cdot \overline{\overline{R}}_i e^{jn\Phi_i} \tag{3.14}$$

4. Induced surface currents

In this section the harmonic surface current densities are defined and the relations between the currents on the different bodies are deduced.

The nth harmonic of the incident field excites a current at $\bar{r}_i$ on S_i of vector surface current density $\bar{J}_{in}^S(\bar{r}_i)$; call this the nth harmonic current. The total current is the sum of the harmonics.

S_i is rotated relative to S_0 through the same angle Φ_i as the field $\bar{E}_n^i(\bar{r}_i)$ is rotated relative to $\bar{E}_n^i(\bar{r}_0)$, see (3.14). Thus, relative to its own orientation, S_i experiences the same incident field harmonic as does S_0, except for the phase factor $e^{jn\Phi_i}$. Therefore the vector currents exhibit the same relations as the fields:

$$\bar{J}_{in}^S(\bar{r}_i) = \bar{J}_{0n}^S(\bar{r}_0) \cdot \bar{\bar{R}}_i e^{jn\Phi_i}. \tag{4.1}$$

(4.1) reveals a major benefit of expressing the field as a sum of harmonics. As the currents on the surfaces are simply related it is necessary to determine the current on only one of them. If the current is found by the moment method to be discussed below, and it is expressed as a set of N unknowns per surface, a direct approach would require the solution of NI equations in NI unknowns, the solution time being asymptotically proportional to $(NI)^3$. With the present approach the solution time is proportional to N^3 per harmonic. We shall presently see that the number of · significant harmonics approximates 2π times the ensemble diameter measured in wavelengths.

5.   The electric field integral equation

In this section we derive the electric field integral equation, the solution of which is the surface current density distributions on the bodies.   It is found necessary to calculate the current on only one body, for only one direction of incidence, and that the currents on the other bodies, for other directions of incidence, may be derived from the first.

The currents induced on the surfaces radiate the scattered field. The total field, incident plus scattered, satisfies the boundary condition that everywhere on the surfaces its tangential component is zero.   This is expressed in an integral equation whose solution is the surface current density distribution.

The field $\overline{E}_n^S(\overline{r})$ at a point of position vector $\overline{r}$ radiated by the nth harmonic currents on all the bodies is the sum

$$\overline{E}_n^S(\overline{r}) = \sum_{\substack{i=0 \\ \overline{r}_i' \text{ on } S_i}}^{I-1} \iint \overline{J}_{in}^S(\overline{r}_i').\overline{\overline{G}}_0(\overline{r},\overline{r}_i')ds' \ , \tag{5.1}$$

where $\overline{\overline{G}}_0(\overline{r},\overline{r})$ is the dyadic Green's function relating the field at $\overline{r}$ to a point source at $\overline{r}$.

With (3.11) and (4.1) this is rewritten in the form

$$\overline{E}_n^S(\overline{r}) = \sum_{i=0}^{I-1} e^{jn\Phi_i} \iint_{\overline{r}_0' \text{ on } S_0} (\overline{J}_{0n}^S(\overline{r}_0').\overline{\overline{R}}_i).\overline{\overline{G}}_0(\overline{r},\overline{r}_0'.\overline{\overline{R}}_i)ds' \tag{5.2}$$

The boundary condition is

$$[\overline{E}_n^i(\overline{r}_j) + \overline{E}_n^S(\overline{r}_j)]_t = 0 \ , \ \text{all } \overline{r}_j \text{ on } S_j, \ j = 0,1,...,I-1 \tag{5.3}$$

where the notation $[.]_t$ specifies the vector component tangential to S_j.

With (3.7) and (5.2), (5.3) becomes

$$[\sum_{i=0}^{I-1} e^{jn\Phi_i} \iint_{\bar{r}_0' \, on \, S_0} (\bar{J}^s_{0n}(\bar{r}_0').\bar{\bar{R}}_i).\bar{\bar{G}}_0(\bar{r}_j,\bar{r}_0'.\bar{\bar{R}}_i)ds']_t$$

$$\tag{5.4}$$

$$= [-E_0 \bar{c}^i_n(\bar{r}_j) e^{jn(\phi_j - \phi^i)}]_t, \quad all \; \bar{r}_j \; on \; S_j, \; all \; j$$

(5.4) must be satisfied for all j. Explicitly for j = 0,

$$[\sum_{i=0}^{I-1} e^{jn\Phi_i} \iint_{\bar{r}_0' \, on \, S_0} (\bar{J}^s_{0n}(\bar{r}_0').\bar{\bar{R}}_i).\bar{\bar{G}}_0(\bar{r}_0,\bar{r}_0'.\bar{\bar{R}}_i)ds']_t$$

$$\tag{5.5}$$

$$= [-E_0 \bar{c}^i_n(\bar{r}_0) e^{jn(\phi_0 - \phi^i)}]_t, \quad \bar{r}_0 \; on \; S_0$$

With (3.11) and (3.13), this may be written, after some rearrangement

$$[\sum_{i=0}^{I-1} e^{jn\Phi_{i+j}} \iint_{\bar{r}_0' \, on \, S_0} \bar{J}^s_{0n}(\bar{r}_0').\bar{\bar{R}}_{i+j}.\bar{\bar{R}}_j^{-1}.\bar{\bar{G}}_0(\bar{r}_0,\bar{r}_i').\bar{\bar{R}}_j ds']_t$$

$$= [-\bar{\bar{E}}_0 \bar{c}^i_n(\bar{r}_j) e^{jn(\phi_j - \phi^i)}]_t, \quad \bar{r}_j \; on \; S_j$$

$$\tag{5.6}$$

where $\bar{\bar{R}}_j^{-1}$ is the dyadic which rotates a vector through the angle $-\Phi_j$ and in which it has been noted that $\Phi_i + \Phi_j = \Phi_{i+j}$ and $\bar{\bar{R}}_i = \bar{\bar{R}}_{i+j}.\bar{\bar{R}}_j^{-1}$.

Using

$$\bar{\bar{R}}_j^{-1}.\bar{\bar{G}}_0(\bar{r}_0,\bar{r}_i')\bar{\bar{R}}_j = \bar{\bar{G}}_0(\bar{r}_j,\bar{r}_{i+j}')$$

$$\tag{5.7}$$

(see Appendix B), and replacing the summation index i by i+j, we obtain

$$[\sum_{i=0}^{I-1} e^{jn\Phi_i} \iint_{\bar{r}_0' \, on \, S_0} \bar{J}^s_{0n}(\bar{r}_0').\bar{\bar{R}}_i.\bar{\bar{G}}_0(\bar{r}_j,\bar{r}_i')ds']_t$$

$$\tag{5.8}$$

$$= [-\bar{\bar{E}}_0 \bar{c}^i_n(\bar{r}_j) e^{jn(\phi_0 - \phi^i)}]_t, \quad \bar{r}_j \; on \; S_j$$

(5.8) is the boundary condition on S_j, Cf. (5.4), and has been derived from (5.5), the boundary condition on the body S_0. Thus satisfying the condition on S_0 satisfies it on all.

In (5.5), multiply both sides by $e^{jn\phi^i}$ and change the order of summation and integration to get

$$[\iint_{\bar{r}_0' \, on \, S_0} \bar{J}_n^s(\bar{r}_0') . \bar{\bar{G}}_\Sigma(\bar{r}_0, \bar{r}_0') ds']_t$$

$$= [-E_0 \bar{c}_n^i(\bar{r}_0) e^{jn\phi_0}]_t, \quad \bar{r}_0 \text{ on } S_0 \qquad (5.9)$$

where

$$\bar{\bar{G}}_\Sigma(\bar{r}_0, \bar{r}_0') = \sum_{i=0}^{I-1} e^{jn\Phi_i} \bar{\bar{R}}_i . \bar{\bar{G}}_0(\bar{r}_0, \bar{r}_0' . \bar{\bar{R}}_i) \qquad (5.10)$$

and

$$\bar{J}_n^s(\bar{r}_0') = \bar{J}_{0n}^s(\bar{r}_0') e^{jn\phi^i} \qquad (5.11)$$

The azimuthal direction of incidence ϕ^i does not appear in (5.9) and hence the new unknown $\bar{J}_n^s(\bar{r}_0')$ is independent of ϕ^i. This is a further benefit of the present approach: if we are interested, as we shall be, in directions of incidence over a range of azimuthal angles ϕ^i, all with the same polar angle θ^i, it is unnecessary to solve more than one integral equation, (5.9). The currents on all bodies, for all azimuthal incidence directions are then, from (4.1) and (5.11),

$$\bar{J}_{in}^s(\bar{r}_i) = \bar{J}_n^s(\bar{r}_0) . \bar{\bar{R}}_i e^{jn(\Phi_i - \phi^i)} \qquad . \qquad (5.12)$$

6.   Surface-fixed   coordinates

Several of the vector quantities of concern to us, such as the $\bar{J}_n^S(\bar{r}_0)$ and both sides of the integral equation to be solved, (5.9), are tangential to the body surfaces.   At a point on the surface the vector may be specified by its components in only two orthogonal directions.   In this section these properties are used to reduce the apparently three-dimensional problem to a two-dimensional one.

For a given problem we define a pair of curvilinear orthogonal coordinates α,β over the surface S_0. This serves to define, at every point $\bar{r}_0$ on S_0 a pair of orthogonal unit vectors $\hat{\alpha}(\bar{r}_0),\hat{\beta}(\bar{r}_0)$ tangential to the surface.   They are related to the cylindrical unit vectors $\hat{\rho},\hat{\phi},\hat{z}$ through the direction cosines

$$\alpha_\rho(\bar{r}_0) = \hat{\alpha}(\bar{r}_0).\hat{\rho}(\bar{r}_0) \,, \ \alpha_\phi = \hat{\alpha}.\hat{\phi} \,, \ \alpha_z = \hat{\alpha}.\hat{z} \,, \ \beta_\rho = \hat{\beta}.\hat{\rho} \,, \ \beta_\phi = \hat{\beta}.\hat{\phi} \,, \ \beta_z = \hat{\beta}.\hat{z}$$

$$(6.1)$$

Note that all the quantities in (6.1), excepting $\hat{z}$, are functions of position, as shown explicitly in the first relation.

Each side of (5.9) is decomposed into its components in the $\hat{\alpha}$ and $\hat{\beta}$ directions:

$$\hat{\alpha}(\bar{r}_0). \iint_{\bar{r}_0' \text{ on } S_0} \bar{J}_n^S(\bar{r}_0').\overline{\overline{G}}_\Sigma(\bar{r}_0,\bar{r}_0')ds' = -E_0 e^{jn\phi_0} c_{n\alpha}^{i\zeta}(\bar{r}_0)$$

$$(6.2)$$

$$\hat{\beta}(\bar{r}_0). \iint_{\bar{r}_0' \text{ on } S_0} \bar{J}_n^S(\bar{r}_0').\overline{\overline{G}}_\Sigma(\bar{r}_0,\bar{r}_0')ds' = -E_0 e^{jn\phi_0} c_{n\beta}^{i\zeta}(\bar{r}_0)$$

where

$$c_{n\eta}^{i\zeta} = \bar{c}_n^{i\zeta}.\hat{\eta} = \begin{bmatrix} c_{n\rho}^{i\zeta} & c_{n\phi}^{i\zeta} & c_{nz}^{i\zeta} \end{bmatrix} \begin{bmatrix} \eta_\rho & \eta_\phi & \eta_z \end{bmatrix}^T \qquad \eta = \alpha,\beta; \zeta = \theta,\phi,$$

$$(6.3)$$

$c_{n\rho}^{i\zeta}, c_{n\phi}^{i\zeta}, c_{nz}^{i\zeta}$ are the cylindrical coordinate components of $\bar{c}_n^{i\zeta}$, $\zeta = \theta,\phi$, i.e., the respective coefficients of $\hat{\rho}$, $\hat{\phi}$, $\hat{z}$ in (3.8) or (3.9), η_ρ $(\eta=\alpha,\beta)$ etc are given by (6.1) and superscript T denotes matrix transposition.

The surface current density $\bar{J}_n^S(\bar{r}_0')$ is also expressed in α and β components $J_{n\alpha}^S$ and $J_{n\beta}^S$ respectively :

$$\bar{J}_n^S(\bar{r}_0') = \hat{\alpha}(\bar{r}_0')J_{n\alpha}^S(\bar{r}_0') + \hat{\beta}(\bar{r}_0')J_{n\beta}^S(\bar{r}_0'). \qquad (6.4)$$

The α and β components are related to the cylindrical components thus:

$$\begin{bmatrix} J_{n\rho}^S \\ J_{n\phi}^S \\ J_{nz}^S \end{bmatrix}_{(\bar{r}_0')} = \begin{bmatrix} \alpha_\rho & \beta_\rho \\ \alpha_\phi & \beta_\phi \\ \alpha_z & \beta_z \end{bmatrix}_{(\bar{r}_0')} \begin{bmatrix} J_{n\alpha}^S \\ J_{n\beta}^S \end{bmatrix}_{(\bar{r}_0')} \qquad (6.5)$$

The subscript on the matrices, here and elsewhere, specifies the arguments of the functions which are its elements.

The integrand in (6.2) may now be written in component form as follows:

$$\bar{J}_n^S(\bar{r}_0') \cdot \overline{\overline{G}}_\Sigma(\bar{r}_0,\bar{r}_0')$$

$$\equiv \begin{bmatrix} G\rho\rho & G\rho\phi & G\rho z \\ G\phi\rho & G\phi\phi & G\phi z \\ Gz\rho & Gz\phi & Gzz \end{bmatrix}_{(\bar{r}_0,\bar{r}_0')} (J_{n\alpha}^S(\bar{r}_0') \begin{bmatrix} \alpha_\rho \\ \alpha_\phi \\ \alpha_z \end{bmatrix}_{(\bar{r}_0')} + J_{n\beta}^S(\bar{r}_0') \begin{bmatrix} \beta_\rho \\ \beta_\phi \\ \beta_z \end{bmatrix}_{(\bar{r}_0')})$$

$$(6.6)$$

The elements of the G matrix, G$\rho\rho$ etc, are derived in Appendix C.

With (6.1) and (6.3) to (6.6), the vector equations (6.2) may now be written in terms of the α,β components:

$$\iint_{\bar{r}_0' \text{ on } S_0} \begin{bmatrix} G\alpha\alpha & G\alpha\beta \\ G\beta\alpha & G\beta\beta \end{bmatrix}_{(\bar{r}_0,\bar{r}_0')} \begin{bmatrix} J_{n\alpha}^S \\ J_{n\beta}^S \end{bmatrix}_{(\bar{r}_0')} ds'$$

$$= -E_0 e^{jn\phi_0} \begin{bmatrix} c_{n\alpha}^{i\zeta} \\ c_{n\beta}^{i\zeta} \end{bmatrix}_{(\bar{r}_0)} \qquad (6.7)$$

where

$$
\begin{bmatrix} G_{\alpha\alpha} & G_{\alpha\beta} \\ G_{\beta\alpha} & G_{\beta\beta} \end{bmatrix}_{(\bar{r}_0, \bar{r}_0')}
$$

$$
= \begin{bmatrix} \alpha_\rho & \alpha_\phi & \alpha_z \\ \beta_\rho & \beta_\phi & \beta_z \end{bmatrix}_{(\bar{r}_0)} \begin{bmatrix} G_{\rho\rho} & G_{\rho\phi} & G_{\rho z} \\ G_{\rho\phi} & G_{\phi\phi} & G_{\phi z} \\ G_{z\rho} & G_{z\phi} & G_{zz} \end{bmatrix}_{(\bar{r}_0, \bar{r}_0')} \begin{bmatrix} \alpha_\rho & \beta_\rho \\ \alpha_\phi & \beta_\phi \\ \alpha_z & \beta_z \end{bmatrix}_{(\bar{r}_0')}
$$

$$(6.8)$$

and as before, $\zeta = \theta, \phi$.

7.   The moment method of solution

The current density distribution is found from the solution of the integral equation (6.7). In this section we describe a method by which this equation may be solved.

Two sets of basis functions, $f_\ell^\alpha(\bar{r}_0)$ and $f_\ell^\beta(\bar{r}_0)$, are defined over S_0 and the current density distributions are expanded in terms of them:

$$J_{n\alpha}^s(\bar{r}_0') = \sum_{\ell=1}^{L_\alpha} a_\ell f_\ell^\alpha(\bar{r}_0') \ , \ J_{n\beta}^s(\bar{r}_0') = \sum_{\ell=1}^{L_\beta} a_\ell f_\ell^\beta(\bar{r}_0') \qquad (7.1)$$

For an exact representation of the currents the summations must in general be infinite. Truncation to the finite lengths L_α, L_β thus implies approximation.

(6.7) and (7.1) give

$$\sum_{\ell=1}^{L_\alpha} a_\ell g_\ell^{\alpha\alpha}(\bar{r}_0) + \sum_{\ell=1}^{L_\beta} b_\ell g_\ell^{\alpha\beta}(\bar{r}_0) = -E_0 e^{jn\phi_0} c_{n\alpha}^{i\zeta}(\bar{r}_0),$$

$$\sum_{\ell=1}^{L_\alpha} a_\ell g_\ell^{\beta\alpha}(\bar{r}_0) + \sum_{\ell=1}^{L_\beta} b_\ell g_\ell^{\beta\beta}(\bar{r}_0) = -E_0 e^{jn\phi_0} c_{n\beta}^{i\zeta}(\bar{r}_0), \qquad (7.2)$$

$$\zeta = \theta \text{ or } \phi$$

where

$$g_\ell^{\eta\chi}(\bar{r}_0) = \iint_{\bar{r}_0' \text{ on } S_0} f_\ell^\eta(\bar{r}_0') G_{\eta\chi}(\bar{r}_0,\bar{r}_0') ds' \qquad \eta = \alpha,\beta; \chi = \alpha,\beta \qquad (7.3)$$

and the alternatives for ζ correspond to the alternative polarisations of the incident field.

The integrand of (7.3) is composed of known functions and hence the integral may be performed, at least numerically. With all the $g_\ell^{\eta\chi}(\bar{r}_0)$ known, (7.2) is now a pair of simultaneous linear equations in the $L_\alpha + L_\beta$ unknowns a_ℓ, b_ℓ. The number of equations can be made equal to the number of unknowns by enforcing (7.2) in $(L_\alpha + L_\beta)/2$ independent ways. The simplest

way to do this is to enforce (7.2) at $(L_\alpha + L_\beta)/2$ different values of $\bar{r}_0$, a technique known as "point matching". A more general technique is to multiply both sides of (7.2) by $(L_\alpha + L_\beta)/2$ independent functions of $\bar{r}_0$ successively, in each case integrating the results over S_0. The use of these weighted integrals gives the technique the name "method of moments". Point matching is an application of the moment method in which the weighting functions are impulses.

A possible choice of basis functions is the set of rooftop functions illustrated in figure 7.1. The surface is divided by the α,β grid into approximately rectangular patches, numbered $\ell = 1,2,...,L$. (We are taking $L_\alpha = L_\beta = L$.) The ℓth function for the current component in the α direction, $f_\ell^\alpha(\bar{r}_0)$, varies with position $\bar{r}_0$ in the patch as a triangle with unit height in the direction of flow α, and as a constant in the transverse (β) direction. The function is zero outside its patch. The function for the β component, $f_\ell^\beta(\bar{r}_0)$, is similar but varying as a triangle in the β direction. The patches overlap such that the edge of each is the centreline of a neighbour except at an edge of a surface.

The overlaps together with the triangularity ensure that the current density is continuous in its flow direction. Also, for a surface of zero thickness terminating in an edge, the normal component of the current density at the edge is zero. In the case where the bodies are in contact and must be separated by a cut, a special basis function must be used at the cut to ensure current continuity there.

If point matching is used, a convenient set of points for its application is the set of points $\bar{r}_{0k}$; $k = 1,2,...,L$, located at the centres of the L patches. Enforcing (7.2) at these points yields the 2L simultaneous linear algebraic equations

$$\sum_{\ell=1}^{L_\alpha} a_\ell g_{k\ell}^{\alpha\alpha} + \sum_{\ell=1}^{L_\beta} b_\ell g_{k\ell}^{\alpha\beta} = -E_0 e^{jn\phi_0} c_{n\alpha}^{i\zeta}(\bar{r}_{0k}),$$

$$\sum_{\ell=1}^{L_\alpha} a_\ell g_{k\ell}^{\beta\alpha} + \sum_{\ell=1}^{L_\beta} b_\ell g_{k\ell}^{\beta\beta} = -E_0 e^{jn\phi_0} c_{n\beta}^{i\zeta}(\bar{r}_{0k}), \qquad (7.4)$$

$$\zeta = \theta \text{ or } \phi$$

where

$$g_{k\ell}^{\eta\chi} = \iint_{\bar{r}_0' \text{ on } S_0} f_\ell^\eta(\bar{r}_0') G_{\eta\chi}(\bar{r}_{0k}, \bar{r}_0') ds' \qquad \eta = \alpha, \beta; \chi = \alpha, \beta \qquad (7.5)$$
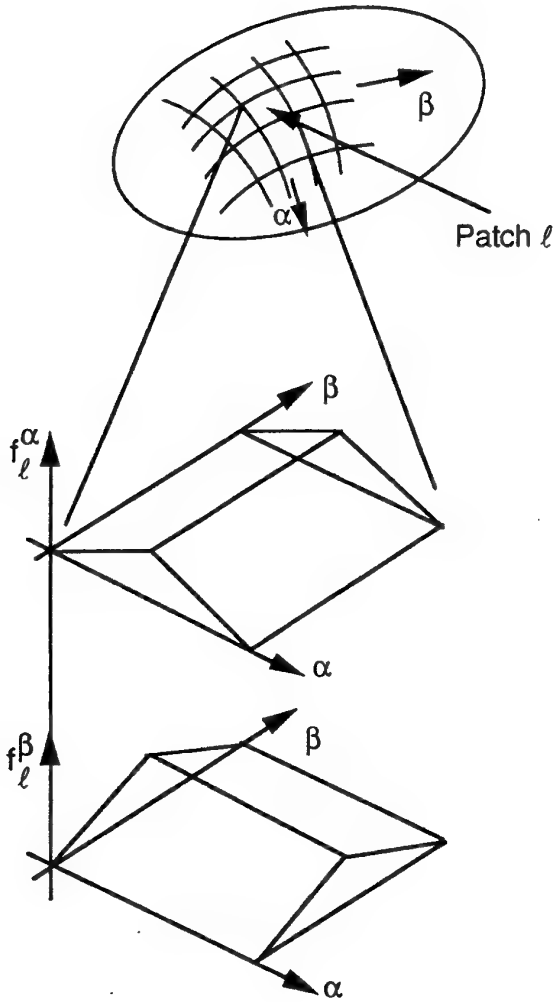

Figure 7.1.   Rooftop functions for representation of the α and β components of the vector current density on patch 1.

8. If the bodies are in contact

In this case there is only one body, with a shape exhibiting angular periodicity. In this section is described the special treatment required for this case.

The original single body is sectored into I separate bodies by cuts exhibiting the same angular periodicity as the original, see figure 8.1 The currents flow on the surface of the original body; there are no currents on the surfaces exposed by the cutting.

Across the lines of the cuts on the original surface the normal component of the current density is continuous. Provided the cut is not along a discontinuity of the surface geometry such as a ridge, the parallel component will be continuous also. Thus in general we take the total vector current density to be continuous across the cuts.

Consider the cut separating bodies 0 and 1 and the current densities at points close to the edges formed by it; let $\bar{r}_{0,e_2}$ be a point on body 0 near its edge 2 and $\bar{r}_{1,e_1}$ be on body 1, near its edge 1, see figure 8.2. The two edges are formed by the cut. In the limit as the points approach the cut and one another, the continuity remarked in the previous paragraph is expressed by

$$\bar{J}^s_{0n}(\bar{r}_{0,e_2}) = \bar{J}^s_{1,n}(\bar{r}_{1,e_1}) \tag{8.1}$$

Now let $\bar{r}_{0,e_1}$ be the point on body 0 corresponding to $\bar{r}_{1,e_1}$ on 1. From (4.1), (5.11) and (8.1) we find

$$\bar{J}^s_n(\bar{r}_{0,e_2}) = \bar{J}^s_n(\bar{r}_{0,e_1}).\overline{\overline{R_1}}e^{jn\Phi_1} \tag{8.2}$$

- in words: the vector current densities on the two cut edges of body 0 differ in direction by angle Φ_1 and in phase by $n\Phi_1$, but are otherwise equal.

This property of the currents may be built into the basis functions so that the solutions exhibit it automatically. For example, a set of rooftop basis functions running from edge 1 to edge 2, see figure 8.3, may include a special function consisting of a half-triangle of strength unity at edge 1, and a second half-triangle of strength

$e^{jn\Phi_1}$ at edge 2. The current described by an expansion in these functions will have the required scalar behaviour. The required vector rotation will be present if the surface directions $\hat{\alpha}(\bar{r}_0), \hat{\beta}(\bar{r}_0)$ rotate from edge to edge through the angle Φ_1 separating the edges in azimuth.

Thus an appropriate choice of basis functions ensures current continuity across the cuts.

It is remarked that the progressive phase shifts of the currents in the separate bodies, see (5.11), ensures that if the ensemble includes the z axis, the currents flowing towards the axis sum to zero at the axis, as required by Kirchhoff's current law.
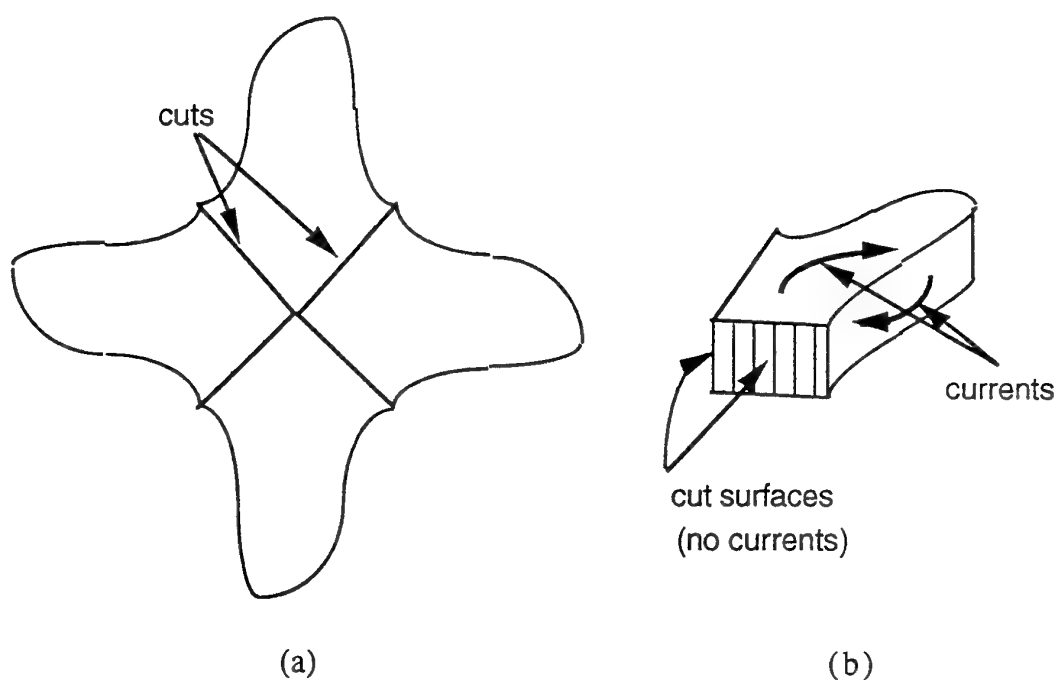
Figure 8.1. (a) "Ensemble" of contacting bodies separated by cuts. (b) One of the separated bodies; no currents flow on the surfaces exposed by the cuts.
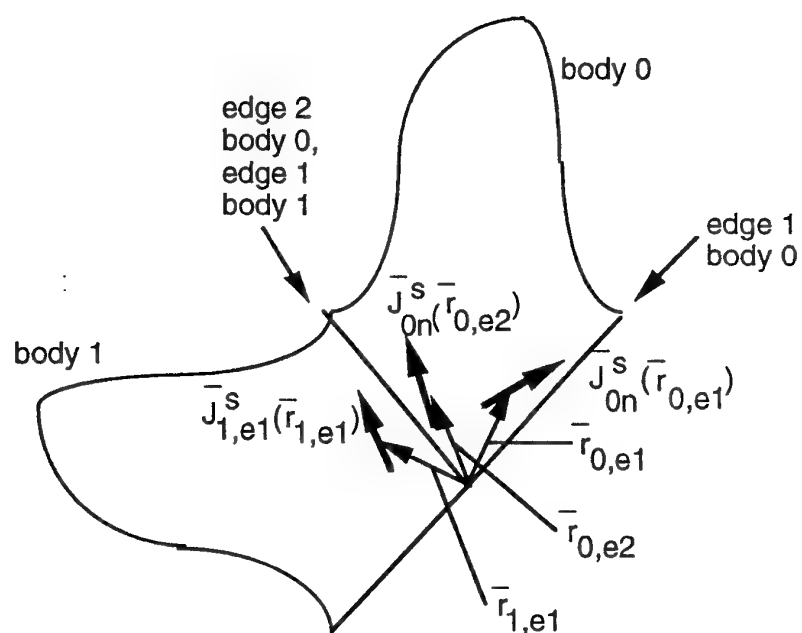

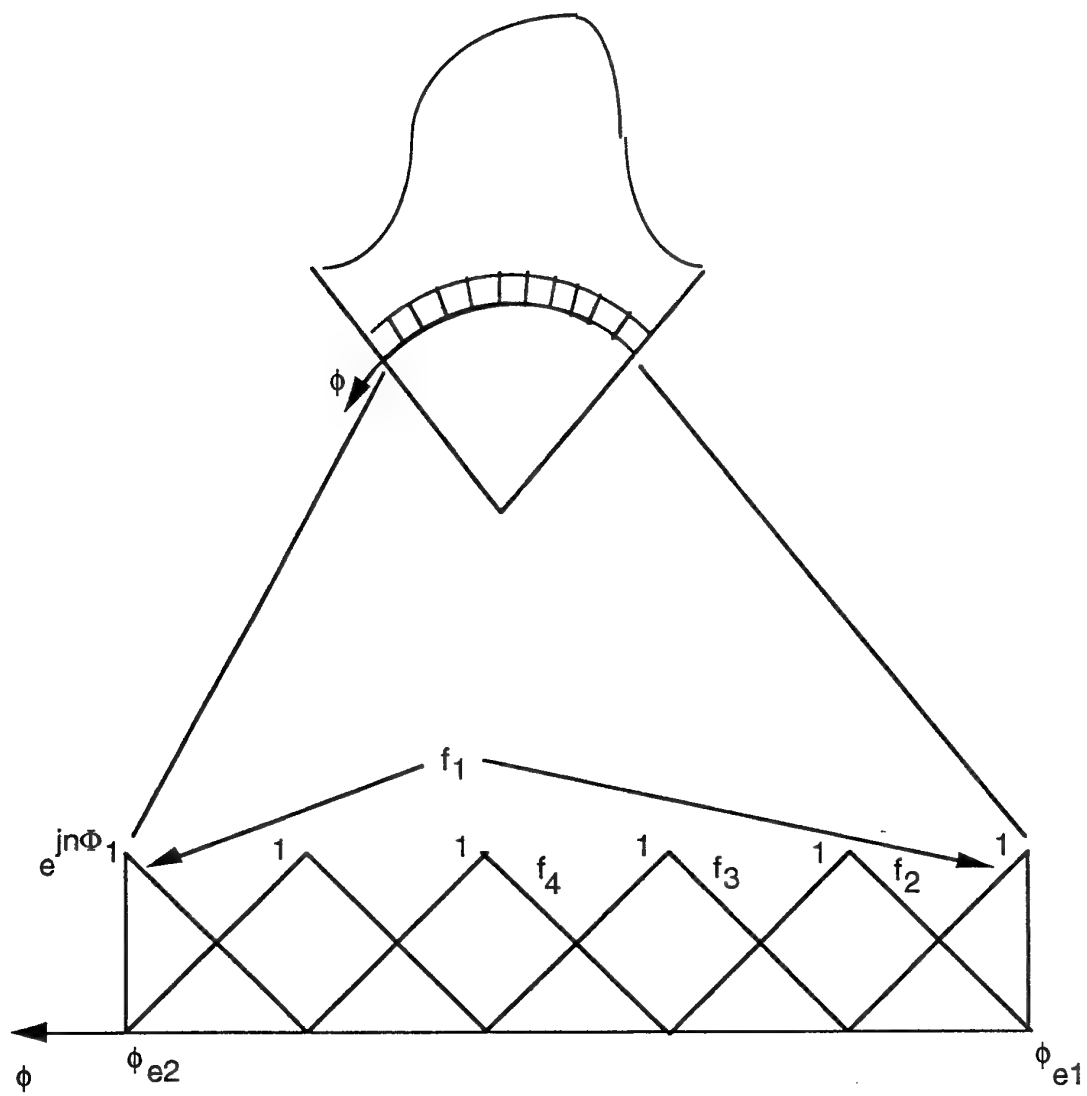Figure 8.2. Showing current densities adjacent to cuts and their continuity across cuts.

Figure 8.3. Rooftop basis functions to enforce continuity across cuts.

9. The scattered field

In this section an expression is found for the field scattered from the stationary ensemble of bodies for given directions of incidence and scatter.

The scattered field at a distant point $\bar{r}^S \equiv (r, \theta^S, \phi^S)$ is the sum of the fields radiated by all the current harmonics on all the bodies; thus from standard radiation theory [e.g. 7],

$$\bar{E}^S(\bar{r}^S) = K_0 \sum_{n=-\infty}^{\infty} \sum_{i=0}^{I-1} \iint_{\bar{r}_i' \text{ on } S_i} \bar{J}^S_{in}(\bar{r}_i').(\hat{\theta}^S\hat{\theta}^S + \hat{\phi}^S\hat{\phi}^S)e^{jk_0\hat{r}^S.\bar{r}_i'}\, ds'$$

(9.1)

where

$$K_0 = jk_0 Z_0 \frac{e^{jk_0 r}}{4\pi r}$$

(9.2)

and Z_0 is the intrinsic impedance of free space.

With (3.11) and (5.12), (9.1) may be written in the form

$$\bar{E}^S(\bar{r}^S) = K_0 \sum_{n=-\infty}^{\infty} \sum_{i=0}^{I-1} e^{jn(\Phi_i - \phi^i)} \iint_{\bar{r}_i' \text{ on } S_i} (A_{n\theta}\hat{\theta}^S + A_{n\phi}\hat{\phi}^S)e^{jk_0 A_r}\, ds'$$

(9.3)

where

$$A_r = \hat{r}^S.(\bar{r}_0'.\overline{\overline{R}}_i), \quad A_{n\theta} = \hat{\theta}^S.(\bar{J}^S_n(\bar{r}_0').\overline{\overline{R}}_i), \quad A_{n\phi} = \hat{\phi}^S.(\bar{J}^S_n(\bar{r}_0').\overline{\overline{R}}_i)$$

(9.4)

By use of (3.12) and the relations among vector components in rectangular, cylindrical and spherical coordinate systems, see Appendix D, the terms in (9.4) may be manipulated to yield

$$A_{n\theta}e^{jk_0 A_r} = \bar{J}^S_n(\bar{r}_0').(\hat{\rho}_0'\cos\theta^S\cos\psi - \hat{\phi}_0'\cos\theta^S\sin\psi - \hat{z}_0'\sin\theta^S)$$
$$e^{jk_0\rho_0'\sin\theta^S\cos\psi}e^{jk_0 z_0'\cos\theta^S}$$

$$(9.5)$$

and

$$A_{n\phi}e^{jk_0A_r} = \bar{J}_n^S(\bar{r}_0').(\hat{\rho}_0'\sin\psi + \hat{\phi}_0'\cos\psi)$$

$$e^{jk_0\rho_0'\sin\theta^S\cos\psi}e^{jk_0z_0'\cos\theta^S}$$

$$(9.6)$$

where

$$\psi = (\phi_0' + \Phi_i - \phi^S) \tag{9.7}$$

and $\hat{\rho}_0', \hat{\phi}_0', \hat{z}_0'$ are unit vectors at $\bar{r}_0'$ in the ρ,ϕ,z directions respectively. ($\hat{z}_0'$ is of course $\hat{z}$, which does not vary with position.)

(9.5) and (9.6) contain products of trigonometric and exponential functions which may be recognised as closely similar to those in (3.4) and (3.5). Their right sides are similarly expanded as Fourier series to give

$$A_{n\eta}e^{jk_0A_r} = \bar{J}_n^S(\bar{r}_0').\sum_{m=-\infty}^{\infty}\bar{c}_m^{S\zeta}(\bar{r}_0')e^{jm(\phi_0'+\Phi_i-\phi^S)} \qquad \zeta = \theta \text{ or } \phi$$

$$(9.8)$$

where $\bar{c}_m^{S\theta}, \bar{c}_m^{S\phi}$ are respectively similar to the $\bar{c}_m^{i\theta}, \bar{c}_m^{i\phi}$ defined in (3.8) to (3.9) with θ^i, ϕ^i replaced by θ^S, ϕ^S and $\bar{r}$ replaced by $\bar{r}_0'$; thus

$$\bar{c}_m^{S\theta}(\bar{r}_0') = j^m(-\hat{\rho}_0'\cos\theta^S j J_m'(P^S) - \hat{\phi}_0'\cos\theta^S\frac{m}{P^S}J_m(P^S) - \hat{z}_0'\sin\theta^S J_m(P^S))$$

$$e^{jk_0z_0'\cos\theta^S}$$

$$(9.9)$$

$$\bar{c}_n^{s\phi}(\bar{r}_0') = -j^m(\hat{\rho}_0' \frac{m}{P^s} J_m(P^s) + \hat{\phi}_0' j J_m'(P^s))e^{jk_0 z_0' \cos\theta^s} \qquad (9.10)$$

where

$$P^s = k_0 \rho_0' \sin\theta^s \qquad (9.11)$$

It will be convenient below to express the vectors $\bar{c}_n^{s\theta}, \bar{c}_n^{s\phi}$ in terms of their α, β components. These are (Cf. (6.3))

$$\begin{bmatrix} c_{n\alpha}^{s\zeta} \\ c_{n\beta}^{s\zeta} \end{bmatrix} = \begin{bmatrix} \alpha_\rho & \alpha_\phi & \alpha_z \\ \beta_\rho & \beta_\phi & \beta_z \end{bmatrix} \begin{bmatrix} c_{n\rho}^{s\zeta} \\ c_{n\phi}^{s\zeta} \\ c_{nz}^{s\zeta} \end{bmatrix}, \qquad \zeta = \theta, \phi \qquad (9.12)$$

where $c_{n\rho}^{s\zeta}, c_{n\phi}^{s\zeta}, c_{nz}^{s\zeta}$ are the cylindrical coordinate components of $\bar{c}_n^{s\zeta}$, i.e., the respective coefficients of $\hat{\rho}, \hat{\phi}, \hat{z}$ in (9.9) for $\zeta = \theta$, or (9.10) for $\zeta = \phi$, and the α_ρ etc are defined in (6.1).

(9.3) with (9.8) to (9.12) becomes after some rearrangement

$$\bar{E}^s(\bar{r}^s) = K_0 \sum_{n=-\infty}^{\infty} \sum_{m=-\infty}^{\infty} e^{-j(n\phi^i + m\phi^s)} \sum_{i=0}^{I-1} e^{j(n+m)\Phi_i}$$

$$\iint_{\bar{r}_0' \text{ on } S_0} \bar{J}_n^s(\bar{r}_0') \cdot (\bar{c}_m^{s\theta}(\bar{r}_0')\hat{\theta}^s + \bar{c}_m^{s\phi}(\bar{r}_0')\hat{\phi}^s)e^{jm\phi_0'} ds' \qquad (9.13)$$

Finally we note from the definition of Φ_i, see (2.1), that the summation on i is zero unless $n + m$ is an integer multiple of I, in which case it equals I. Therefore, set $m = kI - n$ and sum over integer values of k to get

$$\bar{E}^S(\bar{r}^S) = K_0 I \sum_{k=-\infty}^{\infty} \sum_{n=-\infty}^{\infty} e^{jn(\phi^S - \phi^i)}$$

$$\iint\limits_{\bar{r}_0' \, on \, S_0} \bar{J}_n^S(\bar{r}_0') \cdot (\bar{c}_{kI-n}^{S\theta}(\bar{r}_0')\hat{\theta}^S + \bar{c}_{kI-n}^{S\phi}(\bar{r}_0')\hat{\phi}^S)e^{j(kI-n)\phi_0'} ds'$$

$$e^{-jkI\phi^S}$$

$$(9.14)$$

10. The spectrum of the scatter from a rotating ensemble

In this section the hitherto stationary ensemble is considered to rotate about its axis. The scattered field is modulated as the scatterer moves. A formula is found for the spectrum of the modulated field.

Rotation of the ensemble of bodies about the z axis with angular velocity Ω in the ϕ direction may be simulated by setting ϕ^i and ϕ^S in (9.14) to rotate with velocity $-\Omega$ about a stationary ensemble while holding their difference constant. Thus with $\phi^S = -\Omega t$, (9.14) becomes

$$\overline{E}^S(\overline{r}^S) = \sum_{k=-\infty}^{\infty} \overline{E}^S_{kI}(\overline{r}^S) e^{jkI\Omega t} \tag{10.1}$$

where

$$\begin{bmatrix} E^S_{kI,\theta} \\ E^S_{kI,\phi} \end{bmatrix}_{(\overline{r}^S)} = K_0 I \sum_{n=-\infty}^{\infty} e^{jn\Delta\phi}$$

$$\iint_{\overline{r}_0' \, on \, S_0} \overline{J}^S_n(\overline{r}_0') \cdot (\overline{c}^{S\theta}_{kI-n}(\overline{r}_0')\hat{\theta}^S + \overline{c}^{S\phi}_{kI-n}(\overline{r}_0')\hat{\phi}^S) e^{j(kI-n)\phi_0'} \, ds'$$

$$\tag{10.2}$$

and

$$\Delta\phi = (\phi^S - \phi^i) \tag{10.3}$$

is constant.

(10.1) represents a spectrum with lines disposed on each side of zero at intervals of $I\Omega$. This is the radian frequency with which the bodies pass a fixed point; given the focus of this study on the modulation of radar scatter by the blades of a jet engine compressor, $I\Omega$ will be referred to as the "blade rate". Ω will be called the "shaft rate".

$I\Omega$ is also the frequency with which the ensemble re-presents the same aspect to the radar. It is thus the fundamental frequency of the modulation of the scattered field. It is therefore in accord with expectations that the spectral components are separated by $I\Omega$.

(10.1) represents a spectrum centred on zero. If the suppressed factor $e^{j\omega_0 t}$ is reintroduced, the spectrum is centred on the carrier frequency ω_0. An alternative interpretation of (10.1) is that it is the spectrum of the received signal homodyned to base band.

11. The spectrum calculated from the current expansions

For an exact calculation of the spectrum the currents must be known. If they have been found by the methods described in section 6 and 7 and are available in the form of (7.1), then (10.2), with (9.12), may be written as

$$
\begin{bmatrix} E^S_{kI,\theta} \\ E^S_{kI,\phi} \end{bmatrix}_{(\bar{r}^S)} = K_0 I \sum_{n=-\infty}^{\infty} e^{jn\Delta\phi}
$$

$$
(\sum_{\ell=1}^{L_\alpha} a_\ell \iint_{\bar{r}_0' \text{ on } S_0} f_\ell^\alpha(\bar{r}_0') \begin{bmatrix} c^{s\theta}_{kI-n,\alpha} \\ c^{s\phi}_{kI-n,\alpha} \end{bmatrix}_{(\bar{r}_0')} e^{j(kI-n)\phi_0'} ds'
$$

$$
+ \sum_{\ell=1}^{L_\beta} b_\ell \iint_{\bar{r}_0' \text{ on } S_0} f_\ell^\beta(\bar{r}_0') \begin{bmatrix} c^{s\theta}_{kI-n,\beta} \\ c^{s\phi}_{kI-n,\beta} \end{bmatrix}_{(\bar{r}_0')} e^{j(kI-n)\phi_0'} ds')
$$

$$
(11.1)
$$

All the functions and constants in (11.1) are calculable using the methods described in previous sections. This equation is therefore a formal solution for the spectrum of the electomagnetic scatter.

12.   Properties of the spectrum

Sections 10 and 11 have presented formulas from which the spectrum of the scattered field may be calculated.   However, certain general features of the spectrum may be deduced without resort to exact calculation.   These will be described in the present section.

(10.1) reveals the scattered field to consist of a spectrum of frequency components, centred on zero (or ω_0, if the carrier frequency is included), separated by intervals of $I\Omega$ (the blade rate) and extending indefinitely in the positive and negative directions.   This accords with expectations for the periodically modulated field.

Although the spectrum extends indefinitely, only a finite band is significant.   It will now be estimated.

The $\bar{J}_n^s(\bar{r}_0')$ are the solutions of (5.9).   They will be small when the forcing function, the right side, is small.   From (3.8) to (3.10), with the familiar fact that the Bessel function is small when the order exceeds the argument, the right side of (5.9), and hence $\bar{J}_n^s(\bar{r}_0')$, will be small when

$$|n| > k_0 \rho_0 \sin\theta^i \tag{12.1}$$

The largest value of ρ_0 is ρ_{max} , the maximum radius of the ensemble of bodies.   Using this in (12.1) and replacing k_0 by $\dfrac{2\pi}{\lambda_0}$ (where λ_0 is the wavelength at radian frequency ω_0) we have for the maximum value of $|n|$, $|n|_{max}$ say,

$$|n|_{max} = \frac{2\pi}{\lambda_0}\rho_{max}\sin\theta^i \tag{12.2}$$

Multiply both sides by Ω and interpret $|n|_{max}\Omega$ as the frequency separation from the centre, $|\omega|_{max}$ say, of the highest and lowest significant current harmonics.   Thus

$$|\omega|_{max} = \frac{2\pi}{\lambda_0}\rho_{max}\Omega\sin\theta^i \tag{12.3}$$

In the right side of (12.3), $\rho_{max}\Omega\sin\theta^i$ is the maximum velocity of any point on the bodies towards or away from the source of illumination; with the factor $\dfrac{2\pi}{\lambda_0}$ it is recognised as the maximum Doppler shift of the illumination at any point on the bodies.

Thus the currents induced on the bodies consist of a spectrum of frequency components, centred on the illumination frequency ω_0, spaced at intervals of the shaft rate Ω and extending with significant strength to the maximum positive and negative Doppler shifts associated with the linear velocities of the bodies. The spectrum extends indefinitely beyond the Doppler limits but, through the behaviour of the Bessel functions, the strength decreases rapidly.

From the foregoing it is concluded that the integrand of (10.2), due to the factor $\bar{J}_n^S(\bar{r}_0{}')$, is negligible when $|n| > |n|_{max}$ as specified in (12.2).

Through the definitions (9.9) and (9.10) and arguments essentially the same as the foregoing, it is found that the dyadic in (9.14),

$\bar{c}_{kI-n}^{s\theta}(\bar{r}_0{}')\hat{\theta}^S + \bar{c}_{kI-n}^{s\phi}(\bar{r}_0{}')\hat{\phi}^S$, is negligible when

$$|kI - n| > \frac{2\pi}{\lambda_0}\rho_{max}\sin\theta^S \tag{12.3}$$

From this result and (12.1) it is readily found that the maximum value of $|k|$ for which the integrand of (9.14) is non-negligible is

$$|k|_{max} = \frac{2\pi}{I\lambda_0}\rho_{max}(\sin\theta^i + \sin\theta^S) \tag{12.4}$$

Thus $k = \pm|k|_{max}$ give the highest and lowest terms in the summation in (10.1); the spectrum of the scattered field extends above and below the centre by

$$|k|_{max}I\Omega = \frac{2\pi}{\lambda_0}\rho_{max}\Omega(\sin\theta^i + \sin\theta^S) \tag{12.5}$$

which is recognised as the two-way Doppler shift associated with the highest speed, viewed from the source and receiver, of any point on the ensemble of bodies.

$|k|_{max}$ is the number of lines of significant strength on either side of the centre in the spectrum of the scattered field. Under some circumstances (12.4) delivers a $|k|_{max}$ less than one. In this event the scattered field is little, or un-, modulated. Two extreme cases are of interest:

(i) $\theta^i = \theta^S = 0$ (axial backscatter):
(12.4) predicts no spectral lines; despite the approximations used to derive (12.4), this result is rigorously correct, as will be seen below, provided I > 2. Axial backscatter, when the ensemble comprises more than two bodies, is unmodulated.

(ii) $\theta^i = \theta^S = \dfrac{\pi}{2}$ (incidence and scatter in the plane of rotation):
(12.4), with (2.1), predicts

$$|k|_{max} = \frac{4\pi}{I}\frac{\rho_{max}}{\lambda_0} = \frac{\rho_{max}\Phi_1}{\lambda_0/2}$$
$$= d_{max,\lambda/2}$$

(12.6)

where $d_{max,\lambda/2}$ is the maximum chord distance from one body to the next, measured in half-wavelengths.

As derived here (12.6) applies in the case of plane-wave incidence and scatter in the plane of rotation. Radar illumination of jet engines is commonly close to axially incident and (12.6) may appear not to be relevant. However, the field falling on the rotating compressor blades after diffraction through the intake is not a plane wave. It may be decomposed into a spectrum of plane waves which includes components in the plane of rotation. Similarly the scattered field contains components in the plane of rotation.

Thus (12.6) is a significant result for jet engine modulation generally: the number of spectral lines on each side of the centre is approximately equal to the tip-to-tip blade separation measured in half-wavelengths.

If $d_{max,\lambda/2}$ is less than one, there are no significant spectral lines and the scattered field is unmodulated. Here the bodies, even at maximum radius, are separated by less than half a wavelength; the ensemble is electrically similar to a continuous disc.

13. Axial backcatter

This is the case where $\theta^i = \theta^s = 0$. Without loss of generality the incident polarisation may be taken to be $\hat{\theta}^i$.

From (3.8), with Appendix A,

$$\bar{c}_n^{i\theta} = j^n(-\hat{\rho}j\frac{1}{2}(J_{n-1}(0) - J_{n+1}(0)) - \hat{\phi}\frac{1}{2}(J_{n-1}(0) + J_{n+1}(0)))e^{jk_0z}.$$

$$(13.1)$$

But

$$J_n(0) = 1 \qquad n = 0$$
$$\qquad\quad = 0 \qquad n \neq 0$$

and hence

$$\bar{c}_{\pm 1}^{i\theta} = \pm j\frac{1}{2}(\hat{\rho} \pm j\hat{\phi})e^{jk_0z}$$

$$\bar{c}_n^{i\theta} = 0 \qquad n \neq \pm 1$$

$$(13.2)$$

The similarly defined quantities $\bar{c}_n^{s\theta}, \bar{c}_n^{s\phi}$, see (9.9) and (9.10), reduce to

$$\bar{c}_{\pm 1}^{s\theta} = \pm j\frac{1}{2}(\hat{\rho} \pm j\hat{\phi})e^{jk_0z}$$

$$\bar{c}_{\pm 1}^{s\phi} = \mp j\frac{1}{2}(\hat{\rho} \pm j\hat{\phi})e^{jk_0z}$$

$$\bar{c}_m^{s\theta} = \bar{c}_m^{s\phi} = 0 \qquad m \neq \pm 1$$

$$(13.3)$$

It is clear from (5.9) and (13.2) that $\bar{J}_n^s$ is non-zero only for

$$n = \pm 1 \qquad\qquad (13.4)$$

which is therefore a condition for the integrand of (9.14) to be non-zero. With (13.3), a further condition is that

$$kI - n = \pm 1 \qquad\qquad (13.5)$$

(13.4) and (13.5) permit the integrand of (9.15) to be non-zero only with the following combinations of I,n,k:

$$
\begin{array}{llll}
I = 1 & n = -1 & k = -2, 0 \\
& n = +1 & k = \quad 0, +2 \\
I = 2 & n = -1 & k = -1, 0 \\
& n = +1 & k = \quad 0, +1 \\
I = >2 & n = +-1 & k = 0 & \quad\quad (13.6)
\end{array}
$$

From this it is seen that for $I = 1$ and $I = 2$ the values for kI are -2, 0, +2. The spectrum contains components at $\omega_0 - 2\Omega$, ω_0 and $\omega_0 + 2\Omega$.

For $I > 2$ there are no side frequencies; the scattered field is monochromatic at ω_0. The axially backscattered field is unmodulated when the number of bodies is greater than two.

These properties of axial backscatter have been reported previously [7] in a different context.

14.   Calculating the spectrum

In this section are brought together the steps to be followed in numerical calculation of the spectrum.

1.   Define a set of rectangular coordinates with z axis along the axis of the ensemble of bodies.   This serves to define the cylindrical and spherical coordinates also in use.

2.   Choose a single body from the ensemble and call its surface S_0. If the bodies have a common region such as a central hub, a slice of angular width $2\pi/I$ must be cut from it and included with the chosen body. S_0 does not include the surface exposed by the cut.

3.   Define a system of orthogonal curvilinear coordinates α, β on S_0. This serves to define at every point $\bar{r}_0$ on S_0 a pair of orthogonal unit vectors $\hat{\alpha}(\bar{r}_0), \hat{\beta}(\bar{r}_0)$, tangential to the surface.

4.   At every point $\bar{r}_0$ on S_0 determine the direction cosines

$$\alpha_\rho = \hat{\alpha}.\hat{\rho} \; ; \; \alpha_\phi = \hat{\alpha}.\hat{\phi} \; ; \; \alpha_z = \hat{\alpha}.\hat{z} \; ; \; \beta_\rho = \hat{\beta}.\hat{\rho} \; ; \; \beta_\phi = \hat{\beta}.\hat{\phi} \; ; \; \beta_z = \hat{\beta}.\hat{z} \quad .$$

5.   At every point $\bar{r}_0$ on S_0 determine components

$$c_{n\rho}^{i\theta}, \; c_{n\phi}^{i\theta}, \; c_{nz}^{i\theta}, \; c_{n\rho}^{i\phi}, \; c_{n\phi}^{i\phi}, \; c_{nz}^{i\phi} \quad ,$$

see (3.8) to (3.10).

6.   At every point $\bar{r}_0$ on S_0 determine the quantities

$$C_{n\alpha}^\theta = -E_0 e^{jn\phi_0}(c_{n\rho}^{i\theta}\alpha_\rho + c_{n\phi}^{i\theta}\alpha_\phi + c_{nz}^{i\theta}\alpha_z)$$

$$C_{n\beta}^\theta = -E_0 e^{jn\phi_0}(c_{n\rho}^{i\theta}\beta_\rho + c_{n\phi}^{i\theta}\beta_\phi + c_{nz}^{i\theta}\beta_z)$$

$$C_{n\alpha}^\phi = -E_0 e^{jn\phi_0}(c_{n\rho}^{i\phi}\alpha_\rho + c_{n\phi}^{i\phi}\alpha_\phi + c_{nz}^{i\phi}\alpha_z)$$

$$C_{n\beta}^\phi = -E_0 e^{jn\phi_0}(c_{n\rho}^{i\phi}\beta_\rho + c_{n\phi}^{i\phi}\beta_\phi + c_{nz}^{i\phi}\beta_z)$$

(These are needed for solutions for incident polarisation in both the θ and ϕ directions. If only the first (second) is needed, only the first (second) pair of quantities need be calculated.)

7. For every pair of points $\bar{r}_0, \bar{r}_0'$ on S_0 compute the elements of

$$\begin{bmatrix} G_{\rho\rho} & G_{\rho\phi} & G_{\rho z} \\ G_{\phi\rho} & G_{\phi\phi} & G_{\phi z} \\ G_{z\rho} & G_{z\phi} & G_{zz} \end{bmatrix}_{(\bar{r}_0, \bar{r}_0')} .$$

(This is the matrix representation of the dyadic Green's function $\bar{\bar{G}}_\Sigma$, see (C19), Appendix C.)

8. For every $\bar{r}_0, \bar{r}_0$ compute the elements of

$$\begin{bmatrix} G_{\alpha\alpha} & G_{\alpha\beta} \\ G_{\beta\alpha} & G_{\beta\beta} \end{bmatrix}_{(\bar{r}_0, \bar{r}_0')} ,$$

see (6.8).

9. Choose two sets of basis functions,

$$f_\ell^\alpha(\bar{r}_0), \ f_\ell^\beta(\bar{r}_0); \ \ell = 1, 2, ..., L$$

to represent the α and β components, respectively, of the surface current density distributions. (We are here taking equal numbers of the basis functions. This is not strictly necessary.)

10. Choose L values $\bar{r}_{0k}$ of $\bar{r}_0$, with $k = 1, 2, ..., L$. Calculate the elements of the four L x L square matrices

$$g_{k\ell}^{\eta\chi} = \iint f_\ell^\eta(\bar{r}_0')G_{\eta\chi}(\bar{r}_{0k}, \bar{r}_0')ds'$$

in which $\eta\chi$ represent the combinations $\alpha\alpha, \alpha\beta, \beta\alpha, \beta\beta$ and k and ℓ take values $1, 2, ..., L$.

11. Assemble the quantities calculated under headings 6 and 10 in the matrix equation

$$\begin{bmatrix} \left[g_{k\ell}^{\alpha\alpha} \right]_{L \times L} & \left[g_{k\ell}^{\alpha\beta} \right]_{L \times L} \\ \left[g_{k\ell}^{\beta\alpha} \right]_{L \times L} & \left[g_{k\ell}^{\beta\beta} \right]_{L \times L} \end{bmatrix} \begin{bmatrix} a_1 \\ \vdots \\ a_L \\ b_1 \\ \vdots \\ b_L \end{bmatrix} = \begin{bmatrix} C_{n\alpha}^{\zeta}(\bar{r}_{01}) \\ \vdots \\ C_{n\alpha}^{\zeta}(\bar{r}_{0L}) \\ C_{n\beta}^{\zeta}(\bar{r}_{01}) \\ \vdots \\ C_{n\alpha}^{\zeta}(\bar{r}_{0L}) \end{bmatrix}, \quad \zeta = \theta \text{ or } \phi$$

and solve for the constants a_ℓ, b_ℓ, $\ell = 1, 2, \ldots, L$.

The current distribution through its representation by a summation of basis functions, see (7.1), is now known.

12. Compute the integrals

$$\iint\limits_{\bar{r}_0' \text{ on } S_0} f_\ell^\eta(\bar{r}_0') c_{m\eta}^{s\chi}(\bar{r}_0') e^{jm\phi'_0} ds'$$

for the combinations of parameters

$$\eta = \alpha, \beta; \quad \chi = \theta, \phi; \quad |m(\text{integer})| \le \frac{d}{\lambda_0 / 2}.$$

13. Compute the spectral components:

$$\begin{bmatrix} E_{kI,\theta}^s \\ E_{kI,\phi}^s \end{bmatrix}_{(\bar{r}^s)} = K_0 I \sum_{n=-\infty}^{\infty} e^{jn\Delta\phi}$$

$$\left(\sum_{\ell=1}^{L_\alpha} a_\ell \iint\limits_{\bar{r}_0' \text{ on } S_0} f_\ell^\alpha(\bar{r}_0') \begin{bmatrix} c_{kI-n,\alpha}^{s\theta} \\ c_{kI-n,\alpha}^{s\phi} \end{bmatrix}_{(\bar{r}_0')} e^{j(kI-n)\phi_0'} ds' \right.$$

$$\left. + \sum_{\ell=1}^{L_\beta} b_\ell \iint\limits_{\bar{r}_0' \text{ on } S_0} f_\ell^\beta(\bar{r}_0') \begin{bmatrix} c_{kI-n,\beta}^{s\theta} \\ c_{kI-n,\beta}^{s\phi} \end{bmatrix}_{(\bar{r}_0')} e^{j(kI-n)\phi_0'} ds' \right)$$

for all $|kI(\text{integer})| \le \frac{d}{\lambda_0 / 2}.$

If there is interest in the spectrum beyond the Doppler limits, the computations here and under the previous heading should continue beyond the values of m and kI indicated.

15. Conclusions and proposals for further work

Conclusions:

- A theory has been developed by means of which the radar scatter from an ensemble of bodies with angular periodicity, such as a compressor stage of a jet engine, may be calculated.

- The theory exploits the angular periodicity of the scatterer in such a way that the computational load, compared with an approach which does not do this, is reduced by a factor approximately equal to the number of bodies.

- The theory leads to a solution in the form of the spectrum of the scattered field.

- The formal solution, without resort to numerical results, reveals many features of the spectrum such as line separation, bandwidth, number of lines of significant strength etc.

- A numerical approach has been developed in sufficient detail that the equations might be solved by a programmer with little or no familiarity with electromagnetics.

Proposals for Further Work:

The theory described here contemplates the scatterer as an ensemble of bodies in free-space illuminated by a plane wave. The jet engine departs from this ideal model in a number of ways: The engine compressor stage is surrounded by an engine cowling. It is one of several stages close enough together that strong electromagnetic interaction is to be expected. The stages exist in the presence of stator blades which themselves constitute periodic structures. All these departures from the ideal are expected to have their effects on the spectrum.

It is proposed to continue this investigation towards a better understanding of the effects mentioned in the previous paragraph. It is believed that the present theory constitutes a basis for such a continuation.

Appendix A   Formulas involving Bessel functions.

The following formulas or others readily derivable from them are employed at several places in the text. $J_n(\rho)$ is the Bessel function of order n, argument ρ, and $J_n{}'(\rho) = \dfrac{d}{d\rho} J_n(\rho)$.

$$e^{\pm j\rho\cos\phi} = \sum_{n=-\infty}^{\infty} (\pm j)^n J_n(\rho) e^{jn\phi}$$

$$\cos\phi \, e^{\pm j\rho\cos\phi} = \sum_{n=-\infty}^{\infty} (\pm j)^{n-1} J_n{}'(\rho) e^{jn\phi}$$

$$\sin\phi \, e^{\pm j\rho\cos\phi} = \mp \sum_{n=-\infty}^{\infty} (\pm j)^n \frac{n}{\rho} J_n(\rho) e^{jn\phi}$$

$$\frac{n}{\rho} J_n(\rho) = \frac{1}{2}(J_{n-1}(\rho) - J_{n+1}(\rho))$$

$$J_n{}'(\rho) = \frac{1}{2}(J_{n-1}(\rho) + J_{n+1}(\rho))$$

$$J_{-n}(\rho) = (-1)^n J_n(\rho)$$

Appendix B

THIS PAGE LEFT UNINTENTIONALLY BLANK
PLEASE REFER TO AUTHOR

Appendix C   The Dyadic Green's Function for the Periodic Array, $\overline{\overline{G_\Sigma}}$.

By definition of the dyadic Green's function, the field at a point of position vector $\bar{r}$ due to a point source of vector current moment $\bar{p}$ at position $\bar{r}'$ is

$$\overline{E}(\bar{r}) = \bar{p}.\overline{\overline{G_0}}(\bar{r},\bar{r}').$$ (C1)

Express $\overline{E}(\bar{r})$ in terms of its components in the orthogonal coordinate system $\{\eta_1,\eta_2,\eta_3\}$ with unit vectors $\hat{\eta}_1,\hat{\eta}_2,\hat{\eta}_3$ evaluated at $\bar{r}$, thus,

$$\overline{E}(\bar{r}) = \hat{\eta}_1 E_{\eta_1} + \hat{\eta}_2 E_{\eta_2} + \hat{\eta}_3 E_{\eta_3}$$ (C2)

and $\bar{p}$ in terms of the system $\{\zeta_1,\zeta_2,\zeta_3\}$ with unit vectors $\hat{\zeta}_1',\hat{\zeta}_2',\hat{\zeta}_3'$ evaluated at $\bar{r}'$, thus,

$$\bar{p} = \hat{\zeta}_1' p_{\zeta_1'} + \hat{\zeta}_2' p_{\zeta_2'} + \hat{\zeta}_3' p_{\zeta_3'}$$ (C3)

Finally, express (C1) in component form, noting that $E_{\eta_1} = \hat{\eta}_1.\overline{E}(\bar{r})$ etc and $p_{\zeta_1'} = \hat{\zeta}_1'.\bar{p}$ etc, thus:

$$
\begin{bmatrix} \hat{\eta}_1.\overline{E} \\ \hat{\eta}_2.\overline{E} \\ \hat{\eta}_3.\overline{E} \end{bmatrix} =
\begin{bmatrix}
G_{\eta_1\zeta_1'} & G_{\eta_1\zeta_2'} & G_{\eta_1\zeta_3'} \\
G_{\eta_2\zeta_1'} & G_{\eta_2\zeta_2'} & G_{\eta_2\zeta_3'} \\
G_{\eta_3\zeta_1'} & G_{\eta_3\zeta_2'} & G_{\eta_3\zeta_3'}
\end{bmatrix}
\begin{bmatrix} \hat{\zeta}_1'.\bar{p} \\ \hat{\zeta}_2'.\bar{p} \\ \hat{\zeta}_3'.\bar{p} \end{bmatrix}
$$ (C4)

Now let $\bar{p}$ have unit strength and orientations $\hat{\zeta}_1',\hat{\zeta}_2',\hat{\zeta}_3'$ successively to get

$$G_{\eta\zeta'}(\bar{r},\bar{r}') = \hat{\eta}(\bar{r}).\overline{E}(\bar{r};\hat{\zeta}'(\bar{r}'))$$ (C5)

where $\overline{E}(\bar{r};\hat{\zeta}'(\bar{r}'))$ is the field at $\bar{r}$ due to a point dipole at $\bar{r}'$ of unit moment and orientation $\hat{\zeta}'$, and $\eta = \eta_1,\eta_2,\eta_3$; $\zeta = \zeta_1,\zeta_2,\zeta_3$.

From standard radiation theory [e.g. 8] the field of the current distribution $\bar{J}(\bar{r}')$ may be found from the formula

$$\bar{E}(\bar{r}) = \iiint (G'\bar{J}(\bar{r}') + \bar{R}G''\,\bar{R}.\bar{J}(\bar{r}'))dv' \tag{C6}$$

where

$$G'(R) = \frac{1}{j\omega\varepsilon}\frac{1}{4\pi R^3}(-1 - jkR + k^2R^2)e^{-jkR} \quad , \tag{C7}$$

$$G''(R) = \frac{1}{j\omega\varepsilon}\frac{1}{4\pi R^5}(3 + j3kR - k^2R^2)e^{-jkR} \quad , \tag{C8}$$

$$\bar{R} = \bar{r} - \bar{r}' \tag{C9}$$

and the integral is over the volume in which $\bar{J}(\bar{r}')$ is non-zero.

(C6) may be written in dyadic notation:

$$\bar{E}(\bar{r}) = \iiint \bar{J}(\bar{r}').\overline{\overline{G_0}}(\bar{r},\bar{r}')dv' \tag{C10}$$

where

$$\overline{\overline{G_0}}(\bar{r},\bar{r}') = G'\overline{\overline{I}} + G''\overline{RR} \tag{C11}$$

and $\overline{\overline{I}}$ is the identity dyadic.

Let

$$\bar{E} = \bar{E}' + \bar{E}'' \tag{C12}$$

where $\bar{E}'$ and $\bar{E}''$ are the parts associated with G' and G'' respectively in (C10), (C11). Then using (C5) with $\{\eta_1,\eta_2,\eta_3\} = \{\zeta_1,\zeta_2,\zeta_3\} = \{\rho,\phi,z\}$ we have, for the $\rho\rho$ element of the matrix representation of $G'\overline{\overline{I}}$ in cylindrical coordinates,

$$G'_{\rho\rho} = \hat{\rho}.\bar{E}'(\bar{r};\hat{\rho}') = \hat{\rho}.\hat{\rho}'\,G' \tag{C13}$$

where $\hat{\rho}$ and $\hat{\rho}'$ are unit vectors in the ρ directions at $\bar{r}$ and $\bar{r}'$ respectively. Evaluating the dot product in (C13) gives

$$G'_{\rho\rho} = G'\cos(\phi - \phi') \tag{C14}$$

The other elements are found from similar considerations, and are set out as follows:

$$G'\bar{\bar{I}} \equiv G' \begin{bmatrix} \cos(\phi-\phi') & \sin(\phi-\phi') & 0 \\ -\sin(\phi-\phi') & \cos(\phi-\phi') & 0 \\ 0 & 0 & 1 \end{bmatrix} \qquad (C15)$$

Through similar application of (C5) the matrix representation of $G''\overline{RR}$ is found to be

$$G''\overline{RR} \equiv G'' \times$$

$$\begin{bmatrix} (\rho\cos(\phi-\phi')-\rho')(\rho-\rho'\cos(\phi-\phi')) & \rho\sin(\phi-\phi')(\rho-\rho'\cos(\phi-\phi')) & (z-z')(\rho-\rho'\cos(\phi-\phi')) \\ (\rho\cos(\phi-\phi')-\rho')\rho'\sin(\phi-\phi') & \rho\rho'\sin^2(\phi-\phi') & (z-z')\rho'\sin(\phi-\phi') \\ (\rho\cos(\phi-\phi')-\rho')(z-z') & \rho'\sin(\phi-\phi')(z-z') & (z-z')^2 \end{bmatrix}$$

$$(C16)$$

The matrix representation of $\overline{\overline{G_0}}(\bar{r},\vec{r})$, see (C11) is the sum, element by element, of the right sides of (C15) and (C16).

To compute $\overline{\overline{G}}_\Sigma$ in (5.11), consider

$$\bar{p}.\overline{\overline{G}}_\Sigma(\bar{r},\bar{r}_0') = \sum_{i=0}^{I-1} e^{jn\Phi_i} \bar{p}.\overline{\overline{R}}_i.\overline{\overline{G}}_0(\bar{r},\bar{r}_0'.\overline{\overline{R}}_i) \qquad (C17)$$

which is the field at $\bar{r}$ due to the periodic circular array of point dipoles of vector moment $\bar{p}_i = e^{jn\Phi_i}\bar{p}.\overline{\overline{R}}_i$, i=1,2,...I-1, at the corresponding points $\bar{r}_i = \bar{r}_0.\overline{\overline{R}}_i$, see figure C1. Note that

$$\bar{p}_i = e^{jn\Phi_i}(\hat{\rho}(\bar{r}_i')p_\rho + \hat{\phi}(\bar{r}_i')p_\phi + \hat{z}(\bar{r}_i')p_z) \qquad (C18)$$

in which it has been recognised that the unit vectors $\hat{\rho}(\bar{r}_i'), \hat{\phi}(\bar{r}_i'), \hat{z}(\bar{r}_i')$ are related to their values at $\bar{r}_0'$ through the rotation $\overline{\overline{R}}_i$ and the scalars $p_{\rho'}, p_{\phi'}, p_{z'}$ do not vary around the array.

Then with (C15) and (C16), $\overline{\overline{G}}_\Sigma$ may be expressed in matrix form thus

$$\overline{\overline{G}}_\Sigma(\overline{r},\overline{r}_0) \equiv \sum_{i=0}^{I-1} e^{jn\Phi_i} \{G'(R_i) \begin{bmatrix} C_i & S_i & 0 \\ -S_i & C_i & 0 \\ 0 & 0 & 1 \end{bmatrix}$$

$$+ G''(R_i) \begin{bmatrix} (\rho C_i - \rho')(\rho - \rho' C_i) & \rho S_i(\rho - \rho' C_i) & (z-z')(\rho-\rho'C_i) \\ (\rho C_i - \rho')\rho' S_i & \rho\rho' S_i^2 & (z-z')\rho' S_i \\ (\rho C_i - \rho')(z-z') & \rho' S_i(z-z') & (z-z')^2 \end{bmatrix}$$

$$\tag{C19}$$

where

$$C_i = \cos(\phi - \phi_i'), \quad S_i = \sin(\phi - \phi_i') \tag{C20}$$

and

$$R_i = |\overline{r} - \overline{r}_i| = (\rho^2 + \rho_i'^2 - 2\rho\rho_i'\cos(\phi - \phi_i') + (z-z_i')^2)^{\frac{1}{2}} \tag{C21}$$

Since $\rho_i' = \rho_0'$, $\phi_i' = \phi_0' + \Phi_i$, $z_i' = z_0'$, (C21) may be simplified to

$$R_i = (\rho^2 + \rho_0'^2 - 2\rho\rho_0'\cos(\phi - \phi_0' - \Phi_i) + (z-z_0')^2)^{\frac{1}{2}} \tag{C22}$$

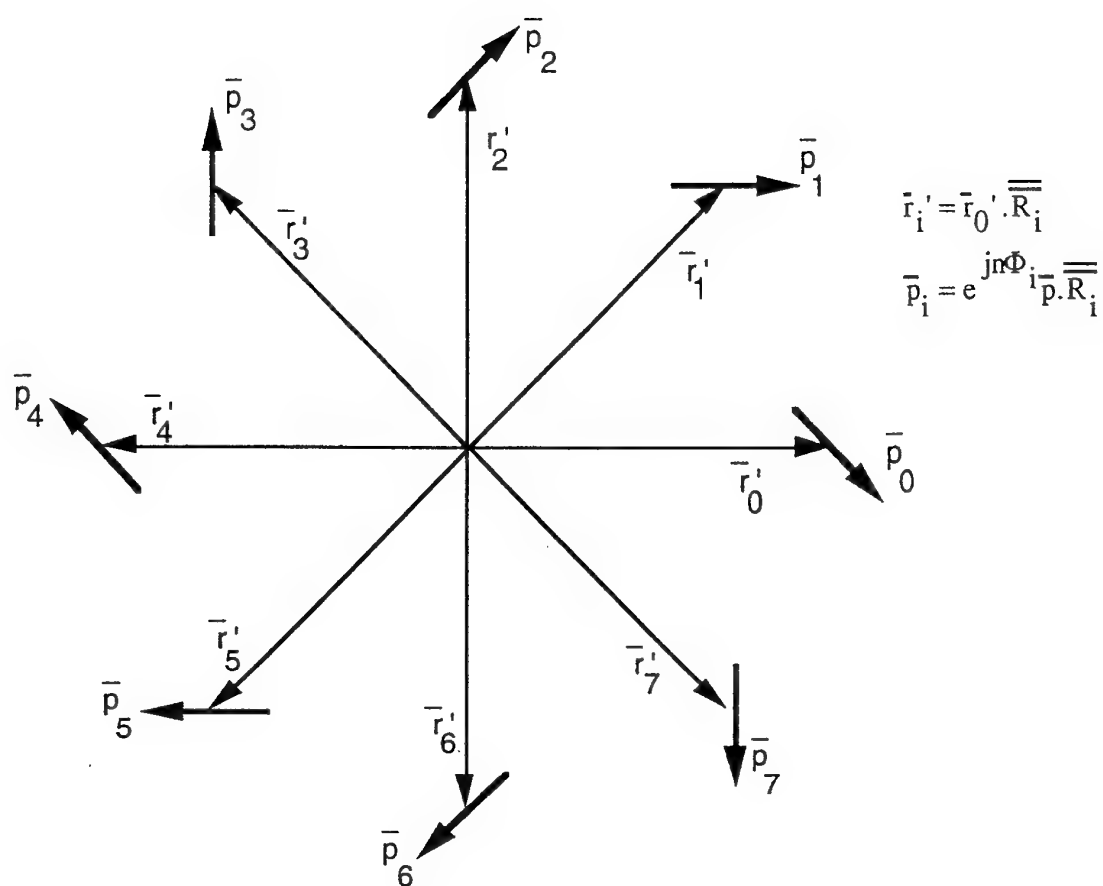$$\bar{r}_i{}' = \bar{r}_0{}' \cdot \overline{\overline{R}}_i$$

$$\bar{p}_i = e^{jn\Phi_i} \bar{p} \cdot \overline{\overline{R}}_i$$

Figure C1: Array of point dipoles $\bar{p}_i$ at corresponding points $\bar{r}_i{}'$.

Appendix D   The expressions $\hat{r}.(\overline{A}.\overline{\overline{R}}), \hat{\theta}.(\overline{A}.\overline{\overline{R}}), \hat{\phi}.(\overline{A}.\overline{\overline{R}})$

$\overline{A}$ is an arbitrary vector, $\overline{\overline{R}}$ is a rotation dyadic of the type defined in (3.12), and (3.12) with rotation angle Φ, and $\hat{r}, \hat{\theta}, \hat{\phi}$ are unit vectors associated with the spherical coordinate system, evaluated at the point (r, θ, ϕ). The unit vectors may be expressed in terms of unit vectors in the rectangular system thus:

$$\hat{r} = \hat{x}\sin\theta\cos\phi + \hat{y}\sin\theta\sin\phi + \hat{z}\cos\theta$$

$$\hat{\theta} = \hat{x}\cos\theta\cos\phi + \hat{y}\cos\theta\sin\phi - \hat{z}\cos\theta \qquad \text{(D1)}$$

$$\hat{\phi} = -\hat{x}\sin\phi + \hat{y}\cos\phi$$

Performing the rotation according to (3.12) on the vector

$$\overline{A} = \hat{x}A_x + \hat{y}A_y + \hat{z}A_z \qquad \text{(D2)}$$

and then forming the dot products with $\hat{r}, \hat{\theta}, \hat{\phi}$ as given in (D1) successively gives

$$\hat{r}.(\overline{A}.\overline{\overline{R}}) = A_x \sin\theta\cos(\phi - \Phi) + A_y \sin\theta\sin(\phi - \Phi) + A_z \cos\theta$$

$$\hat{\theta}.(\overline{A}.\overline{\overline{R}}) = A_x \cos\theta\cos(\phi - \Phi) + A_y \cos\theta\sin(\phi - \Phi) - A_z \sin\theta$$

$$\hat{\phi}.(\overline{A}.\overline{\overline{R}}) = -A_x \sin(\phi - \Phi) + A_y \cos(\phi - \Phi)$$

$$\text{(D3)}$$

Applying the first of (D3) with $\hat{r} = \hat{r}^S \equiv (1, \theta^S, \phi^S)$, $\overline{A} = \overline{r}_0 \equiv (r'_0, \theta'_0, \phi'_0)$ and $\overline{\overline{R}} = \overline{\overline{R}}_i$ with rotation through angle Φ_i, gives, after minor manipulation involving trigonometric identities and the relations between spherical and cylindrical coordinates,

$$\hat{r}^S.(\overline{r}_0.\overline{\overline{R}}_i) = \rho'_0 \sin\theta^S \cos(\phi'_0 + \Phi_i - \phi^S) + z'_0 \cos\theta^S) \qquad \text{(D4)}$$

Now let $\hat{\theta} = \hat{\theta}^S$ and $\overline{A} = \overline{J}^S_n(\overline{r}_0)$, but write the rectangular components of $\overline{A}$ in terms of the cylindrical components of $\overline{J}^S_n$, thus

$$A_x = J^S_{n\rho}(\vec{r}_0)\cos\phi'_0 - J^S_{n\phi}(\vec{r}_0)\sin\phi'_0$$

$$A_y = J^S_{n\rho}(\vec{r}_0)\sin\phi'_0 + J^S_{n\phi}(\vec{r}_0)\cos\phi'_0 \tag{D5}$$

$$A_z = J^S_{nz}(\vec{r}_0)$$

Making these substitutions in the second of (D3) gives

$$\hat{\theta}^S \cdot (\bar{J}^S_n \cdot \bar{\bar{R}}_i) = J^S_{n\rho}\cos\theta^S\cos(\phi'_0 + \Phi_i - \phi^S) - J^S_{n\phi}\cos\theta^S\sin(\phi'_0 + \Phi_i - \phi^S)$$

$$- J^S_{nz}\sin\theta^S$$

$$\tag{D6}$$

Finally, setting $\hat{\phi} = \hat{\phi}^S$, and $\bar{A} = \bar{J}^S_n(\vec{r}_0)$ in the third of (D3) gives the result

$$\hat{\phi}^S \cdot (\bar{J}^S_n \cdot \bar{\bar{R}}_i) = J^S_{n\rho}\sin(\phi'_0 + \Phi_i - \phi^S) + J^S_{n\phi}\cos(\phi'_0 + \Phi_i - \phi^S)$$

$$\tag{D7}$$

References:

1. Morchin W.C.: Airborne Early Warning Radar,1990, Artech House.

2. Skolnik, M.I.: Introduction to Radar Systems, 2nd Ed. 1980, McGraw-Hill.

3. Currie N.C., Brown C.E. (editors): Principles and Applications of Millimeter-Wave Radar, 1987, Artech House.

4. Green H.E.: EM Backscattering from a Helicopter Rotor in the HF Regime, 2nd Australian Symposium on Antennas, CSIRO Radiophysics, Sydney,1989.

5. Cashman J.D., Haack G.: The Radar Backscatter from Turbines Simulated by Wire Structures with Angular Periodicity, Proceedings, 23rd European Microwave Conference, Madrid, 1993, pp987-9.

6. Burke G.J., Poggio A.J.: Numerical Electromagnetic Code (NEC) - Method of Moments, NOSC Technical Document 116, Jan 1981.

7. Chuang C.W., Pathak P.H.: On Wave Modulation by a Rotating Object, IEEE Trans on Antennas and Propagat., vol AP-30, No. 3, May 1982.

8. Balanis C.A.: Advanced Engineering Electromagnetics, Wiley 1989.

The Spectrum of Electromagnetic Scatter from an Angularly Periodic Ensemble of
Bodies Rotating in the Presence of Another Angularly Periodic Ensemble
John Cashman

AUSTRALIA

DEFENCE ORGANISATION

S&T Program
Chief Defence Scientist ⎫
FAS Science Policy ⎬ shared copy
AS Science Corporate Management ⎭
Director General Science Policy Development
Counsellor Defence Science, London (Doc Data Sheet)
Counsellor Defence Science, Washington (Doc Data Sheet)
Scientific Adviser to MRDC Thailand (Doc Data Sheet)
Scientific Adviser Policy and Command
Navy Scientific Adviser (Doc Data Sheet and distribution list only)

Scientific Adviser - Army (Doc Data Sheet and distribution list only)

Air Force Scientific Adviser

Aeronautical and Maritime Research Laboratory
Director

Electronics and Surveillance Research Laboratory
Director (Doc Data Sheet and distribution list only)

Chief of Surveillance Systems Division
Alan Bolton
Author(s):John Cashman

DSTO Library and Archives
Library Fishermans Bend (Doc Data Sheet)
Library Maribyrnong (Doc Data Sheet)
Library Salisbury
Australian Archives
Library, MOD, Pyrmont (Doc Data sheet only)

US Defense Technical Information Center, 2 copies
UK Defence Research Information Centre, 2 copies
Canada Defence Scientific Information Service, 1 copy
NZ Defence Information Centre, 1 copy
National Library of Australia, 1 copy

Capability Systems Staff
Director General Maritime Development (Doc Data Sheet only)
Director General Aerospace Development (Doc Data Sheet only)

Knowledge Staff
Director General Command, Control, Communications and Computers (DGC4) (Doc
Data Sheet only)

Director General Intelligence, Surveillance, Reconnaissance, and Electronic Warfare (DGISREW)R1-3-A142 CANBERRA ACT 2600 (Doc Data Sheet only)
Director General Defence Knowledge Improvement Team (DGDKNIT) R1-5-A165, CANBERRA ACT 2600 (Doc Data Sheet only)

Army
Stuart Schnaars, ABCA Standardisation Officer, Tobruck Barracks, Puckapunyal, 3662(4 copies)
SO (Science), Deployable Joint Force Headquarters (DJFHQ) (L), MILPO Gallipoli Barracks, Enoggera QLD 4052 (Doc Data Sheet only)

Intelligence Program
DGSTA Defence Intelligence Organisation
Manager, Information Centre, Defence Intelligence Organisation

Corporate Support Program
Library Manager, DLS-Canberra

UNIVERSITIES AND COLLEGES
Australian Defence Force Academy
    Library
    Head of Aerospace and Mechanical Engineering
Hargrave Library, Monash University (Doc Data Sheet only)
Librarian, Flinders University

OTHER ORGANISATIONS
NASA (Canberra)
AusInfo
State Library of South Australia
Parliamentary Library, South Australia

OUTSIDE AUSTRALIA

ABSTRACTING AND INFORMATION ORGANISATIONS
Library, Chemical Abstracts Reference Service
Engineering Societies Library, US
Materials Information, Cambridge Scientific Abstracts, US
Documents Librarian, The Center for Research Libraries, US

INFORMATION EXCHANGE AGREEMENT PARTNERS
Acquisitions Unit, Science Reference and Information Service, UK
Library - Exchange Desk, National Institute of Standards and Technology, US
National Aerospace Laboratory, Japan
National Aerospace Laboratory, Netherlands

SPARES (5 copies)

Total number of copies: **46**

DEFENCE SCIENCE AND TECHNOLOGY ORGANISATION DOCUMENT CONTROL DATA		1. PRIVACY MARKING/CAVEAT (OF DOCUMENT)

2. TITLE The Spectrum of Electromagnetic Scatter from an Ensemble of Bodies with Angular Periodicity, as a Model for Jet Engine Modulation	3. SECURITY CLASSIFICATION (FOR UNCLASSIFIED REPORTS THAT ARE LIMITED RELEASE USE (L) NEXT TO DOCUMENT CLASSIFICATION) Document (U) Title (U) Abstract (U)

4. AUTHOR(S) John Cashman	5. CORPORATE AUTHOR Electronics and Surveillance Research Laboratory PO Box 1500 Salisbury SA 5108 Australia

6a. DSTO NUMBER DSTO-GD-0272	6b. AR NUMBER AR-011-713	6c. TYPE OF REPORT General Document	7. DOCUMENT DATE March 2001

8. FILE NUMBER	9. TASK NUMBER	10. TASK SPONSOR DSTO	11. NO. OF PAGES 51	12. NO. OF REFERENCES 8

13. URL on the World Wide http://www.dsto.defence.gov.au/corporate/reports/DSTO-GD-0272	14. RELEASE AUTHORITY Chief, Surveillance Systems Division

15. SECONDARY RELEASE STATEMENT OF THIS DOCUMENT

Approved for public release

OVERSEAS ENQUIRIES OUTSIDE STATED LIMITATIONS SHOULD BE REFERRED THROUGH DOCUMENT EXCHANGE, PO BOX 1500, SALISBURY, SA 5108

16. DELIBERATE ANNOUNCEMENT

No Limitations

17. CASUAL ANNOUNCEMENT	Yes

18. DEFTEST DESCRIPTORS

Radar cross section, Electromagnetic field theory, Electromagnetic fields

19. ABSTRACT

A rotating ensemble of bodies of arbitrary shape with angular periodicity scatters an electromagnetic wave to produce a spectrum of frequency components characteristic of the structure and its rotation. The spectrum and its properties are predicted through electromagnetic field theory.

The theory has been developed such as to exploit the angular periodicity and therefore reduce the computational load by a large factor. A consequence of the approach is that the spectrum is found directly.

Many of the predictions have been confirmed by direct computation of the scattered field for a series of rotational positions to simulate a time series, followed by a discrete Fourier transforming to produce the spectrum.